NASA CONTRACTOR
REPORT

NASA CR-61192

January 1968

NASA CR-61192

REVIEW OF RAWINSONDE REDUCTION METHODS

Prepared under Contract No. NAS 8-5608 by
R. S. Wheeler

THE BOEING COMPANY

For

NASA-GEORGE C. MARSHALL SPACE FLIGHT CENTER
Huntsville, Alabama

January 1968

NASA CR-61192

REVIEW OF RAWINSONDE REDUCTION METHODS

By

R. S. Wheeler

Prepared under Contract No. NAS 8-5608 by

THE BOEING COMPANY

For

Aero-Astrodynamics Laboratory

NASA-GEORG C. MARSHALL SPACE FLIGHT CENTER

ADDENDUM TO NASA CONTRACTOR REPORT

NASA CR-61192

January 1968

REVIEW OF RAWINSONDE REDUCTION METHODS

By

R. S. Wheeler, The Boeing Company

RE: Section 4, "Conclusions and Recommendations," (see Figures 4-2 and 4-3) pp. 4-1 through 4-8

The cyclic variation in the winds depicted in Figures 4-2 and 4-3 of CR 61192 has now been investigated. This error was caused by a problem with the NASA Atmospheric Research Facility's AN/GMD-2A Rawinsonde System, specifically, the comparator, which provides the range measurements. A difficulty in the electromechanical linkage induced a cyclic variation in its turning rate. The periodicity of this variation was shown to be approximately three minutes per cycle, the same as that observed in the reduced GMD-2A winds and balloon rise rates. The problem has now been corrected.

When the AN/GMD-2A equipment at the Mississippi Test Facility was checked, it worked perfectly with no cyclic error present. Apparently, the fault is not common to all GMD-2 sets. It is believed that a bent drive shaft, or other cause of binding, is responsible in those sets which produce these variations.

PREFACE

This document has been prepared by the Post Flight Trajectories Group to satisfy the technical requirements specified by Data Requirement Description SE-665, Exhibit CC, Contract NAS8-5608, Schedule II, Part II, Section A, Task 8.1.7. The task was performed in support of the Aerospace Environment Division, Environmental Applications Branch (R-AERO-YE), with Mr. John Kaufman as the Marshall Space Flight Center Technical Monitor.

ABSTRACT

Rawinsonde reduction techniques oriented specifically for computer operation are reviewed and evaluated. Equations and flow charts are used to facilitate the description of the reduction procedures.

An error study is performed on rawinsonde data to determine accuracies of the tracking and sounding data. An optimal estimation technique is used to compare tracking accuracies of two of the types of rawinsonde systems, the AN/GMD-1, and the AN/GMD-2A systems.

Comparison of various reduction techniques for temperature, humidity, and wind values are made to determine which best suits an accurate, computer-oriented reduction program. Incorporated in this comparison are tests to determine the best technique for digitally filtering the tracking data.

Recommendations are presented in a general fashion in order that the reduction program may be tailored to specific needs and instrumentations.

TABLE OF CONTENTS

ILLUSTRATIONS

APPENDICES

TABLES

SECTION 1

INTRODUCTION

1.0 GENERAL

The Atmospheric Research Facility at Marshall Space Flight Center, NASA, conducts rawinsonde observations aperiodically in connection with far-field sound propogation studies, vehicle engine tests, and other various research requirements. Two types of rawinsonde systems are employed for these observations. One of these is the AN/GMD-1 system, hereafter referred to as the GMD-1, and the other is the AN/GMD-2A, hereafter referred to as GMD-2. GMD-1 employs an AN/AMT-4( ) type of radiosonde and GMD-2 employs an AN/AMQ-9 type of radiosonde. Data acquired from either system is reduced by digital computer to output the thermodynamic and kinematic properties of the atmosphere. The purpose of this report is to review various computer techniques of reduction, evaluate them and to set forth the procedures that give the best results to meet the requirements of the Atmospheric Research Facility.

The coordinate convention of this report differs from that used in most of the documents referenced in this study. Therefore, Paragraph 1.1 of this section is devoted to a definition of the coordinate system, the reason for its use, and its relevance to balloon motion and winds.

This report also includes a study of the errors affecting the data from each system. These errors are determined and the methods of diminishing their effects are discussed. These methods include data editing, smoothing by digital filters, and exclusion of frequency content by altering the rate of sampling. Paragraph 1.2 is added to this section as an aid to the reader by introducing these methods and briefly reviewing the consequences of their usage.

1.1 WIND COORDINATE SYSTEM

The coordinate system used in this report is an orthogonal, curvilinear, nonrotating (earth-fixed) system whose origin is the center of the tracking antenna of the rawinsonde and whose horizontal distances are measured on the surface of the reference sphere. This reference sphere is concentric with an assumed spherical earth, and its radius is the distance from the center of the earth to the center of the antenna. This coordinate system is a modification of "Standard Coordinate System 10 - Earth-Fixed Launch Site" in accordance with the coordinate system standards set forth by NASA for Project Apollo (Reference 1). Winds are defined as the time derivatives of the balloon's displacement on the surface of the reference sphere. Height of the balloon is everywhere measured along radials of the reference sphere and are given in terms of height above sea level simply by adding the height of the antenna above sea level to the height of the balloon above the surface of the reference sphere.

1.1 (CONTINUED)

It should be noted that obtaining winds from the balloon's displacement on the surface of the reference sphere is not in agreement with current procedure which is to refer horizontal displacement to the changing sphere whose surface is always through the centerline of the balloon. This current procedure introduces an error in the winds because of the divergence of radials with increasing height. Utilizing the fixed reference sphere through the antenna eliminates apparent motion due to diverging radials. Hence, the fixed reference sphere has been adopted.

1.2 METHODS TO MINIMIZE DATA ERRORS

Smoothing by digital filters, altering the frequency content of a set of data by changing the sampling rate, and data editing are methods by which data may be treated to minimize the effect of errors contained within the data. Digital filters have the advantage of sharply delineating between disjoint sets of variability when the frequency band limits of these variabilities can be attributed wholly to either significant signal or to the "noise" of random errors. Digital filters also penalize the observations through the loss of data points from each end of the sets of data called observations or rawinsonde runs. Decreasing the sampling rate also costs data points, but the scope of the run remains unchanged. However, the lower sampling rates provide no sharp delineation between frequencies.

Systematic and bias errors are also investigated. Some of these will be detected and corrected in the data editing procedures, but most of them will pass undetected into the data ready for reduction. Unless systematic errors are cyclic, they will not be affected by the application of digital filters nor by changing the sampling rate. If the true variances in measurement of the data are known, the application of estimation theory to overdetermined coordinate positions of the radiosonde transmitter (hereafter referred to as the balloon coordinates - although a slight misnomer) can minimize the variances and optimize the results. Application of estimation theory is discussed and also the means by which the coordinates may be overdetermined.

Variations in the wind reduction procedures are suggested. This paper reports on the results and provides comparisons for an evaluation of these variations. In these comparisons a certain phenomenon observed in wind profiles determined from GMD-2 data is noted. The scope of this paper does not permit a thorough investigation of this phenomenon, but some conjectures as to its cause are presented.

SECTION 2

RAWINSONDE DATA - COMPUTER REDUCTION FORMULAE

2.0 GENERAL

2.1 FORMULAE

For either GMD-1 or GMD-2 raw data, the thermodynamic properties of the atmosphere such as temperature, humidity, vapor pressure and virtual temperature must be calculated to derive the quantities required in the final output. Hence, the formulae and procedures given in this paragraph are common to either GMD-1 or GMD-2 data.

The data editing technique is accomplished by listing the raw data and then visually examining it for logical consistency. Because GMD-1 data are manually keypunched, punching errors can be found and corrected before any data reduction is attempted. GMD-2 data are punched automatically by the Automatic Data Processing unit, so visual examination mainly confirms temperature and humidity inversions by comparison with the record of temperature and humidity ordinates from the recorder. Decreases in slant range are also noted and checked for consistency with changes in elevation angle.

2.1.1 Temperature

Temperature is derived from the ratio of resistance of the temperature element at the baseline temperature to the resistance of the element at the ambient temperature. The baseline temperature is the stabilized temperature in the chamber in which the radiosonde is calibrated and conditioned prior to balloon release. The temperature, t, in degrees Celsius is given by the empirical relationship:

$$t = (170 + t_b)\left\{\frac{R_c}{R_t}\right\}^{0.19} - 170 \qquad (2.1)$$

where t_b is the measured baseline temperature, R_c the resistance of the element at baseline temperature, and R_t the resistance of the element at temperature t. R_c is found by:

$$R_c = \frac{2.137 \times 10^7}{2d_b} - 1.125 \times 10^5 \qquad (2.2)$$

where d_b is the recorder division or ordinate for the temperature in the chamber during the baseline check, and R_t:

$$R_t = \frac{2.137 \times 10^7}{2d_t} - 1.125 \times 10^5 \qquad (2.3)$$

2.1.1 (Continued)

where d_t is the recorder division when the temperature element is at temperature, t. The absolute temperature, T, is given by T = t + 273.15 in degrees Kelvin.

2.1.2 Humidity

The relative humidity is derived for the carbon type sensing element from empirical formulae involving a calculated relative humidity at a temperature of -40°C and corresponding to a humidity ordinate from the recorder of 46 recorder divisions. This calibration humidity, f_c, is derived from the baseline check relationship set into the CP-223A/UM calculator. A preliminary value of relative humidity, f_{40}, is first determined employing different sets of constants dependent on whether the term involving the difference between 46 ordinates and the given humidity ordinate, d_f, is positive or negative. This preliminary humidity is then adjusted by an amount which is a function of the humidity ordinate and the difference between the ambient temperature (in degrees Celsius) and -40°C. Thus the relative humidity, U, is given in percent as follows:

$$U = f_{40} + d_f \left\{ \frac{f_{40} - 33}{1050} \right\} \sqrt{t + 40} \qquad (2.4)$$

and f_{40}, the intermediate value, is derived from:

$$f_{40} = f_c + \left(\left| \frac{46 - d_f}{c} \right| \right)^a (b) \qquad (2.5)$$

when $(46 - d_f) > 0$:

$$a = 1.66 + \frac{46 - d_f}{33}$$

$$b = 100 - f_c$$

$$c = 64.8 - \frac{f_c}{2.51}$$

and when $(46 - d_f) < 0$:

$$a = 0.5 - \left(\frac{46 - d_f}{10} \right)$$

$$b = 10 - f_c$$

2.1.2 (Continued)

$$c = \frac{f_c}{1.45} - 5.198$$

If ambient temperature is colder than -40°C in the formula for U (Equation 2.4), the temperature correction term becomes imaginary. Hence, no temperature correction is applied if the term $(t + 40) \leq 0$, and $U = f_{40}$.

2.1.3 Vapor Pressure

The percent relative humidity of the saturation vapor pressure at any given temperature is the actual partial pressure of the water vapor content of the atmosphere. Based on Teten's empirical formula (Reference 2), the existing vapor pressure, e, is given by:

$$e = \frac{U}{100} (6.11)\ 10^{\{7.5t/(t + 237.3)\}} \qquad (2.6)$$

The constants in the exponent of 10 are those for the vapor pressure over water and are the correct values to use even where the ambient temperature of the atmosphere is below 0° Celsius.

2.1.4 Virtual Temperature

Virtual temperature, T*, is necessary in the determination of the height of the balloon for GMD-1 data reduction, and for the determination of atmospheric pressure in reducing GMD-2 data. It is derived as a function of T, the ambient temperature in degrees Kelvin; pressure, P, in millibars; and the partial pressure, e, of the water vapor in millibars. It is given in degrees Kelvin by the following formula:

$$T^* = T\left(\frac{P}{P - 0.37812e}\right) \qquad (2.7)$$

and the mean virtual temperature, $\bar{T}^*$, for the layer between any data point and the preceding data point:

$$\bar{T}_i^* = \frac{1}{2}(T_i^* + T^*_{i-1})$$

2.2 COORDINATES FROM GMD-1 DATA

The GMD-1 raw data consist of punched cards manually produced from the recorder records. The following information is punched: The elapsed time at half-minute intervals from time of balloon release, the pressure from the pressure calibration chart for the contact indicated, the recorder chart ordinate for the temperature, the ordinate for the humidity, the antenna elevation and azimuth angles for the rawin recorder to the nearest

2.2 (CONTINUED)

tenth of a degree. Preceding the cards giving this data for each time point in a rawinsonde run is an identification card punched with certain necessary information. Tables 2-I and 2-II show the information content necessary for the reduction procedures recommended in this report for GMD-1 and GMD-2 data.

TABLE 2-I. RECOMMENDED GMD-1 ID AND RAW DATA CARD CONTENT

ID DATA CARD	
Column	Type of Information
1, 2	Day of Month
3	Blank
4, 5	Month of Year
6	Blank
7, 8	Last Two Numbers of the Year
9	Blank
10, 11, 12, 13	Time (GMT) Zulu
14	Blank
15, 16, 17, 18, 19	Station Number
20	Blank
21, 22, 23	F_c from Computer CP-223B/UM
24	Blank
25, 26, 27	Surface Wind Direction, Degrees
28	Blank
29, 30, 31	Surface Wind Speed, (Tenth) mps
32	Blank
33, 34, 35	Surface Temperature, (Tenth) Degrees Celsius
36	Blank
37, 38, 39	Surface Humidity, Percent
40	Blank
41, 42, 43	Baseline Temperature, (Tenth) Degrees Celsius
44	Blank
45, 46, 47	Baseline Temperature Ordinate (Tenth)

2.2 (CONTINUED)

TABLE 2-I. (CONTINUED)

RAW DATA CARD	
Column	Type of Information
1, 2, 3	Time in Minutes
4	Decimal Point
5	Time in Tenth/Minutes
6	Comma
7, 8, 9, 10	Pressure, mb
11	Decimal Point
12	Pressure, mb (Tenth)
13	Comma
14, 15	Temperature Ordinate
16	Decimal Point
17	Temperature Ordinate (Tenth)
18	Comma
19, 20	Humidity Ordinate
21	Decimal Point
22	Humidity Ordinate (Tenth)
23	Comma
24, 25	Elevation Angle (Degrees)
26	Decimal Point
27	Elevation Angle (Tenth) (Degrees)
28	Comma
29, 30, 31	Azimuth Angle (Degrees)
32	Decimal Point
33	Azimuth Angle (Tenth) (Degrees)
34	Comma

2.2 (CONTINUED)

TABLE 2-II. RECOMMENDED GMD-2 ID AND RAW DATA CARD CONTENT

ID DATA CARD	
Column	Type of Information
1, 2	Day of Month
3	Blank
4, 5	Month of Year
6	Blank
7, 8	Last Two Numbers of the Year
9	Blank
10, 11, 12, 13	Time (GMT) Zulu
14	Blank
15, 16, 17, 18, 19	Station Number
20	Blank
21, 22, 23	F_c from Computer CP-223/UM
24	Blank
25, 26, 27, 28, 29	Surface Pressure, (Tenth) mb
30	Blank
31, 32, 33, 34	Surface Wind Direction, Degrees
35	Blank
36, 37, 38, 39	Surface Wind Speed, (Tenth) mps
40	Blank
41, 42, 43	Surface Temperature Ordinates (Tenth)
44	Blank
45, 46, 47	Surface Humidity Ordinates (Tenth)
48	Blank
49, 50, 51	Surface Temperature, (Tenth) Degrees Celsius
52	Blank
53, 54, 55	Surface Humidity, Percent
56	Blank
57, 58, 59	Baseline Temperature, (Tenth) Degrees Celsius
60	Blank
61, 62, 63	Baseline Temperature Ordinate (Tenth)

2.2 (CONTINUED)

TABLE 2-II. (CONTINUED)

RAW DATA CARD	
Column	Type of Information
1, 2, 3, 4	Time in Seconds
5	Blank
6, 7, 8, 9, 10, 11	Slant Range, Meters
12	Blank
13, 14, 15, 16	Elevation Angle (Hundredth) (Degrees)
17	Blank
18, 19, 20, 21, 22	Azimuth Angle (Hundredth) (Degrees)
23	Blank
24, 25, 26	Temperature Ordinate (Tenth)
27	Blank
28, 29, 30	Humidity Ordinate (Tenth)
31 Thru 77	Blank
78	If 0, No Lost Signal
79	If 0, No Lost Sequence
80	Card Registering Character

2.2.1 GMD-1 Balloon Height

The basic dimension for reduction of the balloon coordinates and winds from GMD-1 data is the balloon height. This height, actually the height of the radiosonde instrument, is derived from the integration of the hydrostatic equation by incremental additions of the thicknesses of layers between data points. These thicknesses are determined in geopotential meters from the pressures given at each data point and the arithmetic mean value of the virtual temperatures at these points delineating the layers in accordance with the following formula (Reference 3):

$$\Delta\phi_i = 29.2897959\ \bar{T}_i^*\ \ln\left(\frac{P_{i-1}}{P_i}\right) \qquad (2.9)$$

2.2.1 (Continued)

Then the height at each data point above the surface is given in geopotential meters by:

$$\phi_n = \sum_{i=1}^{n} \Delta\phi_i \qquad (2.10)$$

which needs no correction for curvature of the earth. Conversion of geopotential height to geometric height is done using two constants r´ and R* whose values are dependent on latitude of the station. The formula for conversion to geometric height is:

$$X' = \frac{R^*\phi}{r' - \phi} \qquad (2.11)$$

X, the height above sea level is then:

$$X = X' + H$$

2.2.2 GMD-1 Balloon Coordinates

The horizontal-distance-out, HDO, of the balloon from the antenna is determined by means of the formula (Reference 4):

$$HDO = (R_H + X') \cos\left[E + \sin^{-1}\left(\frac{R_H \cos E}{R_H + X'}\right)\right] \qquad (2.12)$$

where R_H is the sum of R_E, the local radius of the earth, plus H, the height of the antenna above sea level; and where E is the elevation angle indicated by the antenna. The geometry for this equation can easily be seen by referring to Figure 2-1.

The curvilinear coordinates in the Y (positive to the east) and Z (positive to the north) directions are readily obtained from the following formulae:

$$Y = R_H \sin^{-1}\left(\frac{HDO \sin A}{R_H + X'}\right) \qquad (2.13)$$

and,

$$Z = R_H \sin^{-1}\left(\frac{HDO \cos A}{R_H + X'}\right) \qquad (2.14)$$

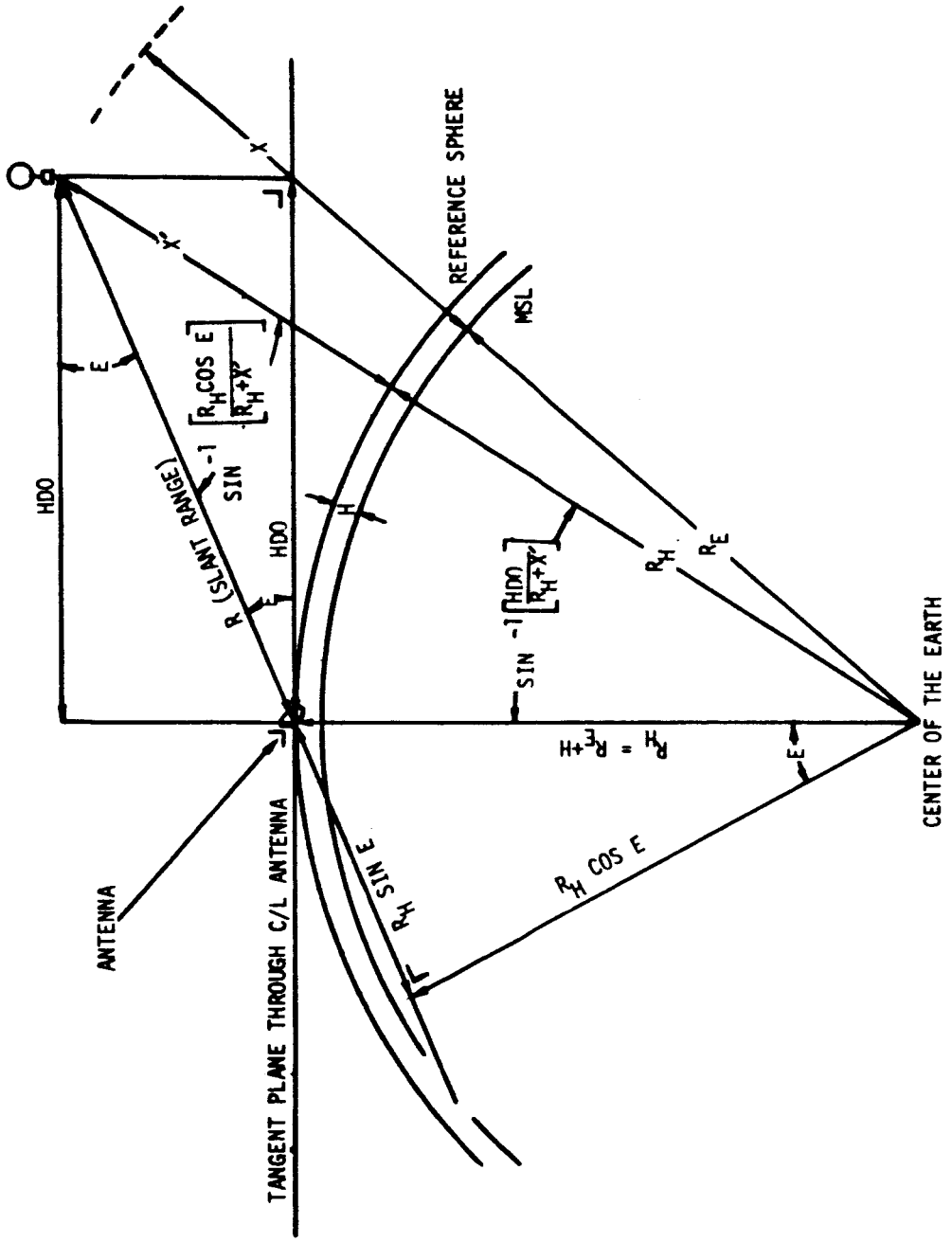

FIGURE 2-1. COORDINATE TRANSFORMATIONS FOR THE COMPUTATION OF HEIGHT, X, AND HORIZONTAL DISTANCE OUT, HDO

2.2.2 (Continued)

where

$$R_H = R_E + H$$

and A is the azimuth angle measured by the antenna clockwise from true north in the tangent plane. These curvilinear coordinates are the values as would be measured on the surface of the reference sphere which is centered at the center of the earth and whose radius, R_H, is the radius of the earth, R_E, plus the height of the antenna, H, above mean sea level.

2.3 COORDINATES AND PRESSURE REDUCTION - GMD-2

GMD-2 raw data are automatically punched as received from the AN/AMQ-9 radiosonde by the Automatic Data Processing (ADP) unit. The data cards for each time point including zero, the balloon release time, and each five seconds thereafter to the termination of the run contain the following information: the time elapsed since release in seconds, the measured slant range to the balloon, the elevation angle to the nearest hundredth of a degree, the azimuth angle to the nearest hundredth of a degree, recorder division ordinates for temperature and humidity. The thermodynamic properties of temperature, humidity, and vapor pressure are determined in computerized reduction identically to the procedures set forth in paragraph 2.1 except that both the temperature and humidity ordinates read from the data cards must be multiplied by a factor of 0.95 to make them equivalent to the recorder divisions indicated on the recorder. These adjusted ordinate values may then be reduced by the formulae thus far presented.

Data necessary for calculating the winds are directly measured by the GMD-2 system: R, the slant range; E, the elevation angle; and A, the azimuth angle. The one parameter missing, but necessary to a complete description of the atmosphere, is pressure. This must be determined from the balloon geometric height coordinate readily determined from R and E.

2.3.1 Height of Balloon

The determination of the height of the balloon above the tangential plane through the antenna is not significant nor is this the coordinate required. Rather, it is the height above the reference sphere through the antenna. Solution for this height, as can be seen in Figure 2-1, is given by the following formula involving the law of cosines and functions of R, slant range, and E, elevation angle (Reference 3):

$$X' = [R_H^2 + R^2 + 2RR_H \sin E]^{\frac{1}{2}} - R_H \qquad (2.15)$$

2.3.1 (Continued)

where $R_H = R_E + H$, as before the sum of the local radius of the earth and the height of the antenna above sea level. From this height, pressure at each data point can be determined.

2.3.2 Pressure

The height X' is converted to geopotential height by the reverse process of converting the geopotential to geometric height as was done with GMD-1 data. The formula involving the same latitude dependent constants r' and R^* is:

$$\phi = \frac{X' r'}{R^* + r'} \tag{2.16}$$

Since height is determined for each data point, the geopotential height is thus known for each data sample.

In reducing this data to determine the pressure, an approximation of the pressure is first determined in order to correct the temperature profile to virtual temperature. Beginning with the known surface pressure, P_o, the following formulae are used (Reference 3):

$$P_{a_i} = P_{a_{i-1}} \text{ EXP } \left[\frac{\phi_{i-1} - \phi_i}{14.64489795\ (T_{i-1} + T_i)}\right] \tag{2.17}$$

where $P_{a_{i=0}} = P_o$ for the initial calculation. Then virtual temperature is very closely approximated for the level of P_{a_i} by:

$$T^* \cong \frac{TP_a}{P_a - 0.37812e} \tag{2.18}$$

and

$$P_i = P_{i-1} \text{ EXP } \left[\frac{\phi_{i-1} - \phi_i}{14.64489795\ (T^*_{i-1} + T^*_i)}\right] \tag{2.19}$$

2.3.3 GMD-2 Balloon Coordinates

Because slant range, R, is directly measured, the horizontal-distance-out (HDO) of the balloon measured along the tangent plane is:

$$HDO = R \cos E$$

2.3.3 (Continued)

Using this parameter as was done with GMD-1 data, the curvilinear coordinates of Y and Z are similarly determined:

$$Y = R_H \sin^{-1}\left(\frac{HDO \sin A}{R_H + X'}\right) \tag{2.13}$$

and

$$Z = R_H \sin^{-1}\left(\frac{HDO \cos A}{R_H + X'}\right) \tag{2.14}$$

2.4 COMPUTATION OF ADDITIONAL THERMODYNAMIC PROPERTIES

Several other thermodynamic quantities are computed to produce a complete reduction of the raw data. Since these all are functions of atmospheric properties already reduced from GMD-1 and GMD-2 raw data, the formulae are applicable to either type of data reduction.

2.4.1 Pressure

Pressure is sometimes required in units other than the meteorological unit of millibars. In units of kilogram (weight) per square meter:

$$P' = 10.1971621\ P \tag{2.20}$$

In units of newtons per square meter:

$$P'' = 10^2\ P \tag{2.21}$$

2.4.2 Density

Density, ρ, in kilograms per cubic meter is determined by:

$$\rho = 0.3483832\ \frac{P}{T^*} \tag{2.22}$$

In units of kilograms (weight) $sec^2 m^{-4}$, density is

$$\rho' = 0.0355252\ \frac{P}{T^*} \tag{2.23}$$

In units of newtons $sec^2 m^{-4}$, density is

$$\rho'' = 34.83832\ \frac{P}{T^*} \tag{2.24}$$

2.4.3 Optical Index of Refraction

The optical index of refraction is given in "N" units by (Reference 3):

$$N = (n - 1)\ 10^6 = 77.54 \frac{P}{T} + 37.84 \frac{e}{T^2} \times 10^4 - 9.66 \frac{e}{T} \quad (2.25)$$

where n is the true index of refraction, a dimensionless ratio slightly greater than 1.0.

2.4.4 Electromagnetic Index of Refraction

The index of refraction for radar frequencies is given in "N" units by (Reference 3):

$$N = (n - 1)\ 10^6 = 77.6 \frac{P}{T} + 37.3256 \frac{e}{T^2} \times 10^4 \quad (2.26)$$

where n is the dimensionless ratio representing the actual index of refraction.

2.4.5 Speed of Sound

The speed of sound, C_s, with respect to the medium - the atmosphere - is given in meters per second by (Reference 5):

$$C_s = 20.0467\ (T^*)^{1/2} \quad (2.27)$$

If the velocity of sound in the atmosphere with respect to a fixed point on the earth is required, the component of wind in the direction of interest must be added to C_s.

2.4.6 Coefficient of Viscosity

The coefficient of viscosity, μ, is given in newton sec m^{-2} by (Reference 5):

$$\mu = \frac{1.458 \times 10^{-8}\ (T)^{3/2}}{T + 110.4} \quad (2.28)$$

2.5 WIND REDUCTION

With the computation of the balloon coordinates from either GMD-1 or GMD-2 data, reduction into wind components can be accomplished with simple differentiation with respect to time by dividing the displacement by the time interval from point Q_{i-1} to Q_{i+1}. The simplest differentiating

2.5 (CONTINUED)

filter accomplishes this identically by multiplying three successive coordinate values by $-f_s/2$ for Q_{i-1}, 0.0 for Q_i, $f_s/2$ for Q_{i+1}, and applying the sum of the products to the Q_i data point (f_s is the sampling frequency in samples per second). However, such simple differentiation must assume some treatment of the raw data to eliminate errors of the accidental, systematic, and random types that exist in the data. Prior to discussion of this preliminary treatment of the raw data, the reduction of component winds into the resultant wind vector will be set forth.

Simple differentiation with respect to time of the Y and Z coordinate gives the wind components toward the east and north, respectively. The winds, however, in normal meteorological convention are specified in direction by that azimuth from which they blow and the wind direction is given by that angle measured clockwise from true north. Therefore, the wind direction is determined by the following means from the acute angle D between the wind axis of flow and the local meridian. D is given in magnitude by:

$$D = \tan^{-1} \left| \frac{\dot{Y}}{\dot{Z}} \right| \tag{2.29}$$

where $\dot{Y}$ is the E-W wind component - positive to the east - and is the time derivative of the E-W displacement. Similarly $\dot{Z}$ is the N-S wind component - positive to the north - and is the time derivative of the N-S displacement of the balloon. Wind direction W_D is then specified by the following quadrant dependence on whether $\dot{Y}$ and $\dot{Z}$ are positive, negative, or zero:

If $\dot{Y}$ is + and $\dot{Z}$ is +, $W_D = D + 180°$

If $\dot{Y}$ is - and $\dot{Z}$ is +, $W_D = 180° - D$

If $\dot{Y}$ is - and $\dot{Z}$ is -, $W_D = D$

If $\dot{Y}$ is + and $\dot{Z}$ is -, $W_D = 360° - D$

If $\dot{Y}$ is 0 and $\dot{Z}$ is +, $W_D = 180°$

If $\dot{Y}$ is 0 and $\dot{Z}$ is -, $W_D = 360°$

If $\dot{Y}$ is 0 and $\dot{Z}$ is 0, $W_D = 0$ (Calm)

If $\dot{Y}$ is + and $\dot{Z}$ is 0, $W_D = 270°$

If $\dot{Y}$ is - and $\dot{Z}$ is 0, $W_D = 90°$

2.5 (CONTINUED)

The magnitude of the wind vector is wind speed, W_s, and is easily determined from:

$$W_s = \left[(\dot{Y})^2 + (\dot{Z})^2\right]^{1/2} \qquad (2.31)$$

A profile of the winds aloft plotted against either time of the data point or equivalent equal altitude increments will show a variability that is not necessarily representative of the true wind field depending on the maximum frequency or wave number content permitted by the time or height spacing of the data points. Therefore, some smoothing process is needed to treat the data.

With GMD-1 data, the sampling rate is normally (at MSFC) one per 30 seconds. In height spacing, this is about one sampling per 150 meters. The maximum frequency or wave number content of the data is, therefore, one cycle per minute or about one per 300 meters. Periodicities and wave lengths of this order of magnitude must be largely, if not completely, attributable to the variability of the atmospheric structure. From this fact, it is submitted that smoothing of the raw data to eliminate random or systematic cyclical errors is not valid. Despite this, it should be noted that the differentiating process over two data intervals to determine $\dot{Y}$ or $\dot{Z}$ for the central data point is, in its very nature, a smoothing procedure which eliminates all of the maximum frequency content and corrupts every lower frequency.

Even without filtering, the sampling rate of GMD-1 could afford to be increased and still have a content in cyclic and random variability that would be attributable mainly to the winds. Dependent on feasibility of trying to manually punch data cards at a more rapid rate, it is recommended that the sampling rate be increased to one per fifteen seconds which permits a minimum wave length at the termination frequency of 150 meters.

With GMD-2 data, the sampling rate of one per five seconds or about one per 25 meters of height allows a maximum frequency of one cycle per ten seconds or maximum wave number content averaging about one cycle per 50 meters. Certainly, variability in the data of this frequency cannot be attributed to the true wind structure because of the self-imposed lateral motions of the balloon dynamics and the lack of response capabilities of the balloon and train to such rapid cyclic variability in the wind. Therefore, applying a smoothing filter to the raw data from the GMD-2 system is very much in order.

The optimum filter, as explained in Appendix C, for applying to the GMD-2 raw data is one of the Martin type constrained smoothing filters. The recommended procedure is to apply this smoothing to the raw data after editing to correct accidental errors. This is to be done before any reduction or operations involving slant range, elevation, and azimuth angles. The exception, of course, is in trying to apply any smoothing to raw data

2.5 (CONTINUED)

such as temperature and humidity ordinates. Smoothing these would conceal or obliterate real and radical changes in the normal lapse rates of these parameters which can be quite sharp edged and exist in relatively thin layers.

The design for the filter required for GMD-2 data is one which passes wave lengths greater than 150 meters and cuts off all shorter wave lengths. A simple solution could be achieved by decreasing the sampling rate to one per fifteen seconds which would accomplish what is the recommended sampling rate for GMD-1 also. Incidentally, this would also eliminate the apparent step function measurement of temperature and humidity ordinates because it would permit the clock-driven commutator of the AMQ-9 to call in updated ordinates before the next data card is automatically punched.

In the following section, the logic and data flow charts of the computer reduction techniques for GMD-1 and GMD-2 data are presented. Together with the formulae set forth in this section, these will aid the engineer and the programmer in developing a reduction program in keeping with the recommendations of this document.

SECTION 3

FLOW CHARTS FOR RAWINSONDE PROGRAMS

3.0 GENERAL

To aid the engineer and programmer in developing a computer program to reduce either GMD-1 and GMD-2 rawinsonde data, data flow charts are presented in this section. Only the logic of the data flow is presented since further detail of the program will vary with the computer and the programming language used. Furthermore, only difficult areas and those that differ between data sets are represented in any detail.

3.1 GMD-1 DATA FLOW CHART

The data flow chart for the atmospheric parameters that are necessary to carry the computation of GMD-1 data through the wind values is presented in Figure 3-1. This flow chart develops the data flow logic by displaying the necessary inputs to an equation that computes a certain parameter. For example, it is not possible to compute relative humidity until the temperature has been computed. In turn, all that is necessary to compute the temperature is the temperature recorder division, d_t. Each equation necessary to compute these values can be found in Section 2. In addition, the techniques to compute the balloon coordinates and wind values are not discussed since a detailed flow of the computation for these values can be found in Appendix C.

3.2 GMD-2 DATA FLOW CHART

The data flow chart for the atmospheric parameters that are necessary to carry the computation of GMD-2 data through the wind values is presented in Figure 3-1.

The significance of Figure 3-1 is that logic differences exist because of differences in input data. For either set of rawinsonde data, computation through vapor pressure is identical. For GMD-1 data, geometric height (or altitude) is a result of integrating the hydrostatic equation, given the virtual temperature profile. Height for the GMD-2 data, however, is a direct result of Equation 2-17 because slant range is provided.

Whereas pressure is directly measured in the GMD-1 system, it must be computed in the GMD-2 system. This is one of the major differences between the two systems and their reduction programs. To reverse the "pressure-to-altitude" procedure of the GMD-1 system, it is necessary to have virtual temperature from the GMD-2 data. This, obviously, cannot be computed since its equation, Equation 2.7, requires pressure. It is, therefore, necessary to estimate this pressure by using the normal atmospheric temperature, as computed by Equation 2.1, as input into the pressure computation to yield an approximated pressure. This approximated pressure is used to compute virtual temperature which in turn is used to compute the actual pressure at the level in question.

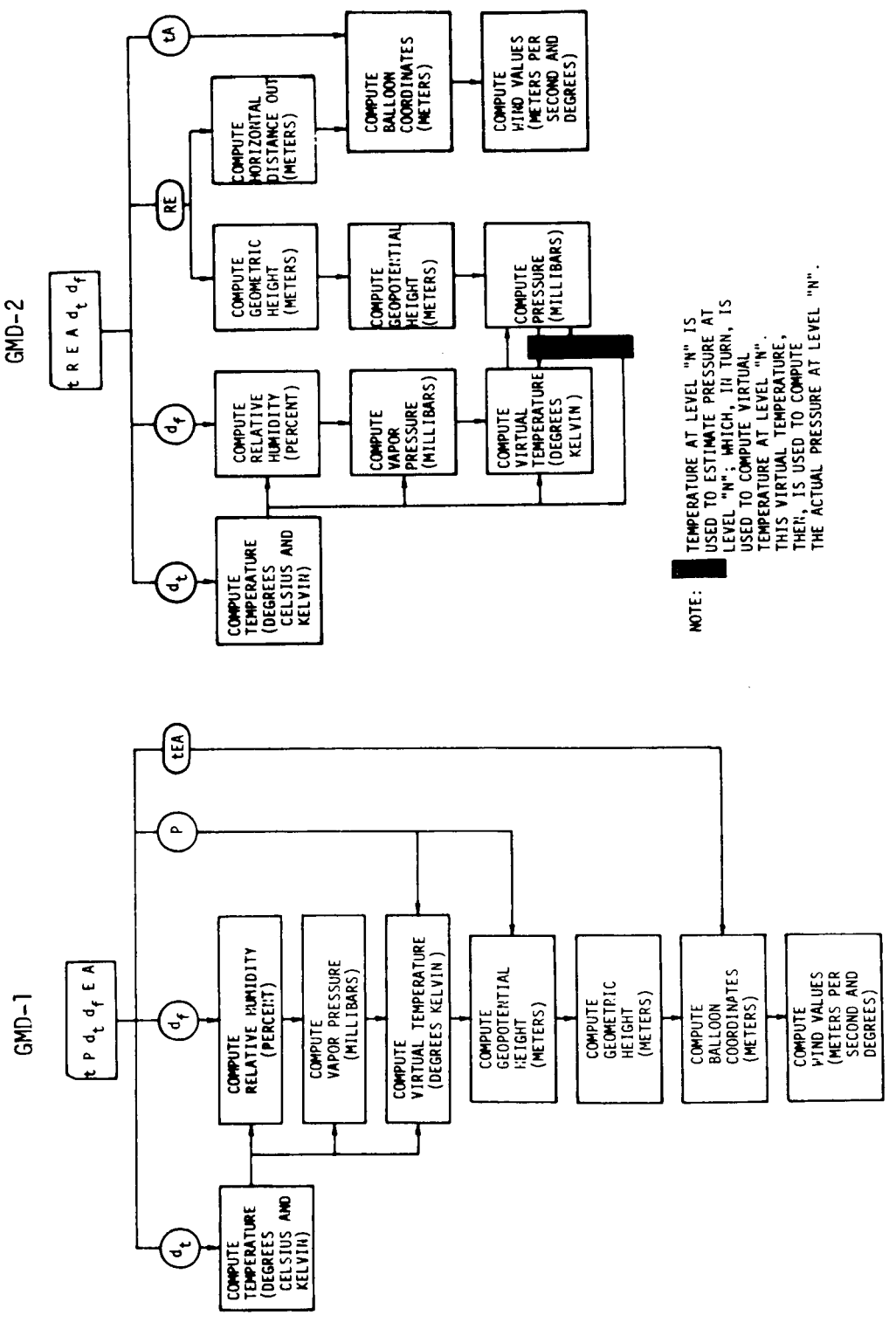

FIGURE 3-1. PROGRAM DESCRIPTION FOR RAWINSONDE REDUCTION

3.2 (CONTINUED)

The only other difference between the two charts in Figure 3-1 is in the computation of horizontal distance out using slant range and elevation values as inputs for GMD-2 data. This same parameter is a function of the geometric height and elevation angles for GMD-1 data and falls within the scope of computation of balloon coordinates.

Other atmospheric parameters, i.e., density, speed of sound, etc., are identical for both reduction programs, and follow the computations presented in Section 2.4. For this reason, they are not included.

SECTION 4

CONCLUSIONS AND RECOMMENDATIONS

4.0 CONCLUSIONS

In Appendix B, alternative approaches to the reduction of meteorological data are reviewed and critiqued. In cases where alternatives exist either in formulae or procedures, the methods presented in Section 2 are those selected because they produce more logically consistent and accurate results. However, if reduction results showed no significant difference, the formula or technique presented in Section 2 is the simpler and more easily programmed method. This is true also of the alternative methods of determining the winds reviewed and discussed in Appendix C. The most suitable wind reduction method is the third presented which is tabbed for identification purposes as MOD-3. It, briefly, is the procedure currently used at MSFC; of first smoothing the raw data, then transforming them into the orthogonal curvilinear coordinates of the balloon position at each time interval, and then differentiating the coordinates to compute the wind components.

The discussion in the previous sections and in the Appendices to this report have left a few unanswered questions. For instance, in the use of filters for smoothing, the optimum filter type is recommended but no particular set of filter weights are named. The question as to how much wind data can one afford to lose because of the number of filter weights employed is purposely unanswered since the winds between the surface and the first available fully filtered point must either be derived by the "educated" guess of a linear interpolative scheme from the known surface wind to the level of the first calculated wind or by the use of expanding span filters from the initial level to the full span selected. The interpolative scheme could be performed by computer but should then be modified by a meteorologist for the effects expected due to the observed thermal structure between the levels being interpolated. The use of a series of digital filters with expanding span can also be accomplished by computer and would produce more objective results than the alternate method. Furthermore, the reverse of the same series of filters providing a contracting span could be used at the terminal end of the rawinsonde run. Use of one of these techniques must be weighed against the advantage of a large span (large number of weights) for use on the central portions of the data sequence. The larger the number of weights used in a filter, the more precisely can the frequencies, comprised chiefly of noise, be delineated from those properly attributable to signal in any set of data. The sharper the roll-off interval between a defined cutoff frequency and a desired termination frequency, the greater is the number of filter weights required to stay within a given accuracy bound (Reference 6). It is, therefore, desirable to have as large a span within reason as possible. This can be seen in the frequency response curves shown in Figure 4-1 for a 13-weight and a 73-weight filter. The number of weights in a Martin filter is a function only of the frequency interval between the cutoff frequency and the termination frequency and independent of what the desired cutoff or termination frequency may be.

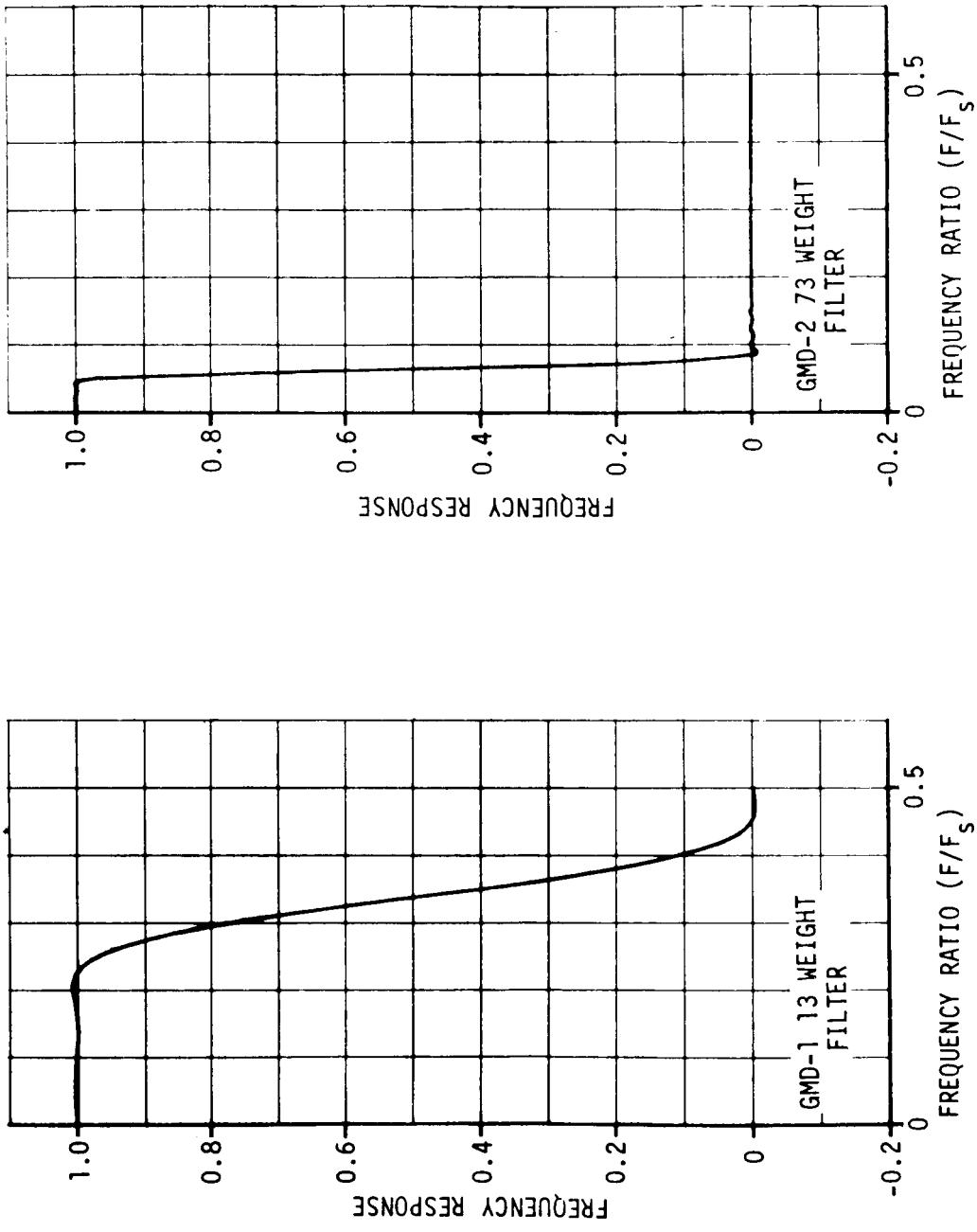

FIGURE 4-1. FREQUENCY RESPONSES OF GMD-1 (13 WEIGHT) AND GMD-2 (73 WEIGHT) FILTERS

4.0 (CONTINUED)

Another unanswered question is the cause of the large systematic cyclic changes in the rate of rise indicated by the GMD-2 data as depicted in Figure 4-2 which occurs in phase with a considerable cyclic change in the magnitude of the wind vector even when the data are preliminarily smoothed with the stringent 73-weight filter depicted in Figure 4-1. At first it was thought that this correlation between the horizontal and vertical accelerations was evidence of vertical motions of the atmosphere either associated with vertical wind shear or with gravity waves imposed by local topography. However, as is observed, the vertical rise rates and horizontal accelerations determined from the simultaneously observed GMD-1 data show little or no correlation with each other and reveal practically none of the larger cyclic changes of the GMD-2 data. This eliminates the probability that the approximately 200 second periods of the cycles in the GMD-2 data were due either to wind structure or some systematic characteristic of the balloon's buoyancy and drag dynamics. It, therefore, appears to be some characteristic of the GMD-2 tracking and ranging system. The same simultaneous data from which the speeds in Figures 4-2 and 4-3 were determined were used in the calculations for the optimization of balloon coordinates by application of estimation theory depicted in Figures 4-4 and 4-5 (see Appendix A). Examination of these figures show that the changes of slope of the height-time curve and the time-HDO curve for the GMD-2 data are remarkably synchronous with the indicated vertical and horizontal speeds shown in Figure 4-2 for the GMD-2 data. This, at first thought, would certainly be anticipated. However, it must be understood that the elevation angles used in GMD-1 calculations for the optimization by estimation theory are the elevation angles measured by the GMD-2 antenna, and the time-HDO curve from the GMD-1 computations shows relatively small and random changes of slope uncorrelated with the undulations of the GMD-2 curves. This leads to the conclusion that the 200-second cyclic changes in the GMD-2 curve are due to some as yet undetermined cyclic and phenomenal error in the ranging measurements by the GMD-2 system since they are not present in the elevation angle data.

4.1 RECOMMENDATIONS

The recommendations most pertinent to the purpose of this document which can improve the quality of rawinsonde reduction refer to the sampling rate and the punching of elevation and azimuth angle data on the input data cards. As indicated in the paragraph on wind reduction in Section 2, it appears that increasing the sampling rate of GMD-1 data to one per fifteen seconds would better delineate signal from noise in the frequency domain. It is, therefore, recommended that the possibility of doing this without increasing the number of accidental errors and without jeopardizing the accurate transposing of the data to punched cards be investigated; and that if the higher sampling rate appears feasible, it be made a part of the standard operating procedure for computerized reduction of GMD-1 rawinsonde runs.

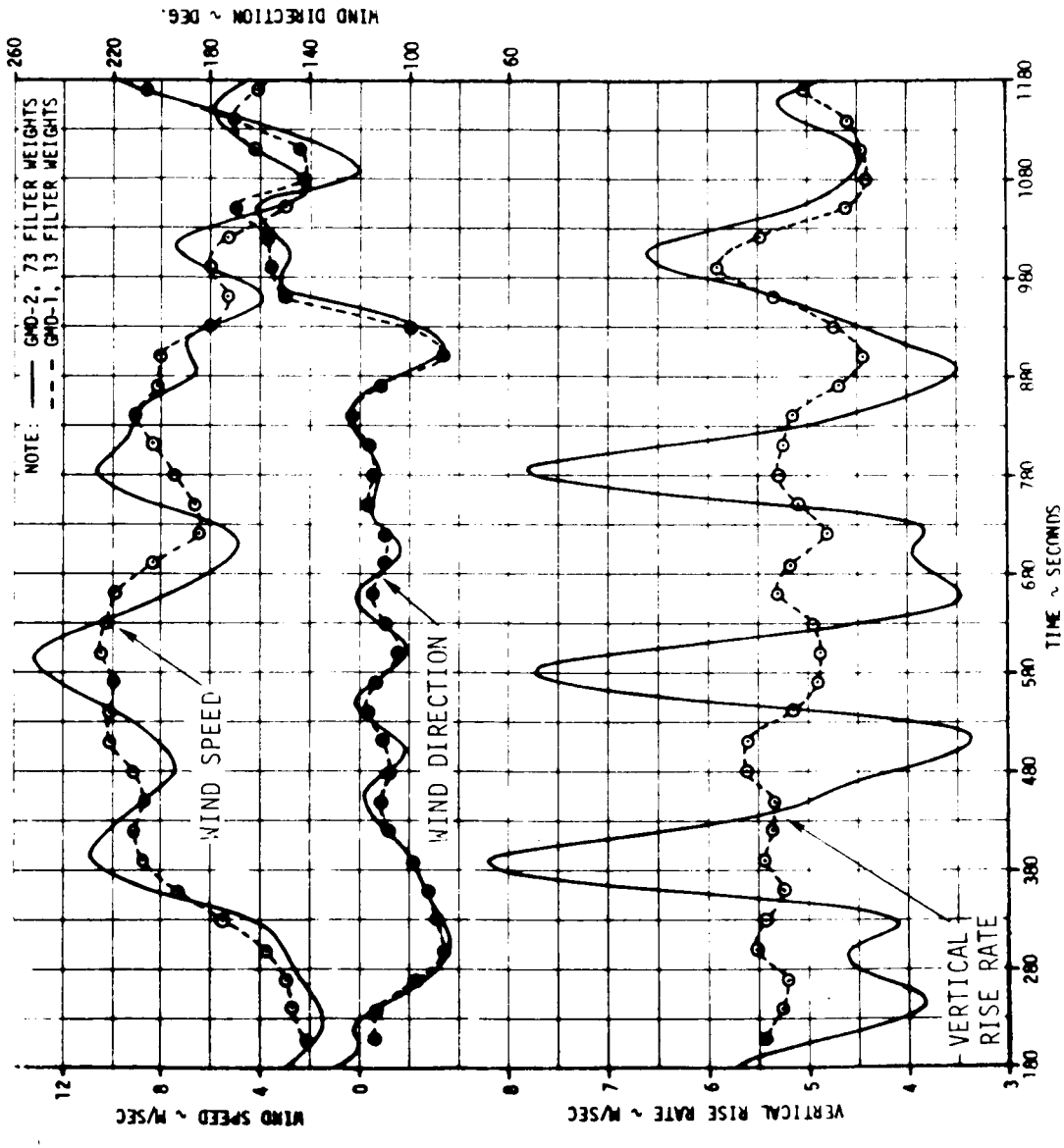

FIGURE 4-2. SIMULTANEOUSLY DETERMINED WINDS - SMOOTHED SPEED, DIRECTION AND VERTICAL RISE RATES - 1754 GMT, SEPTEMBER 6, 1967 - GMD-1 AND GMD-2 DATA

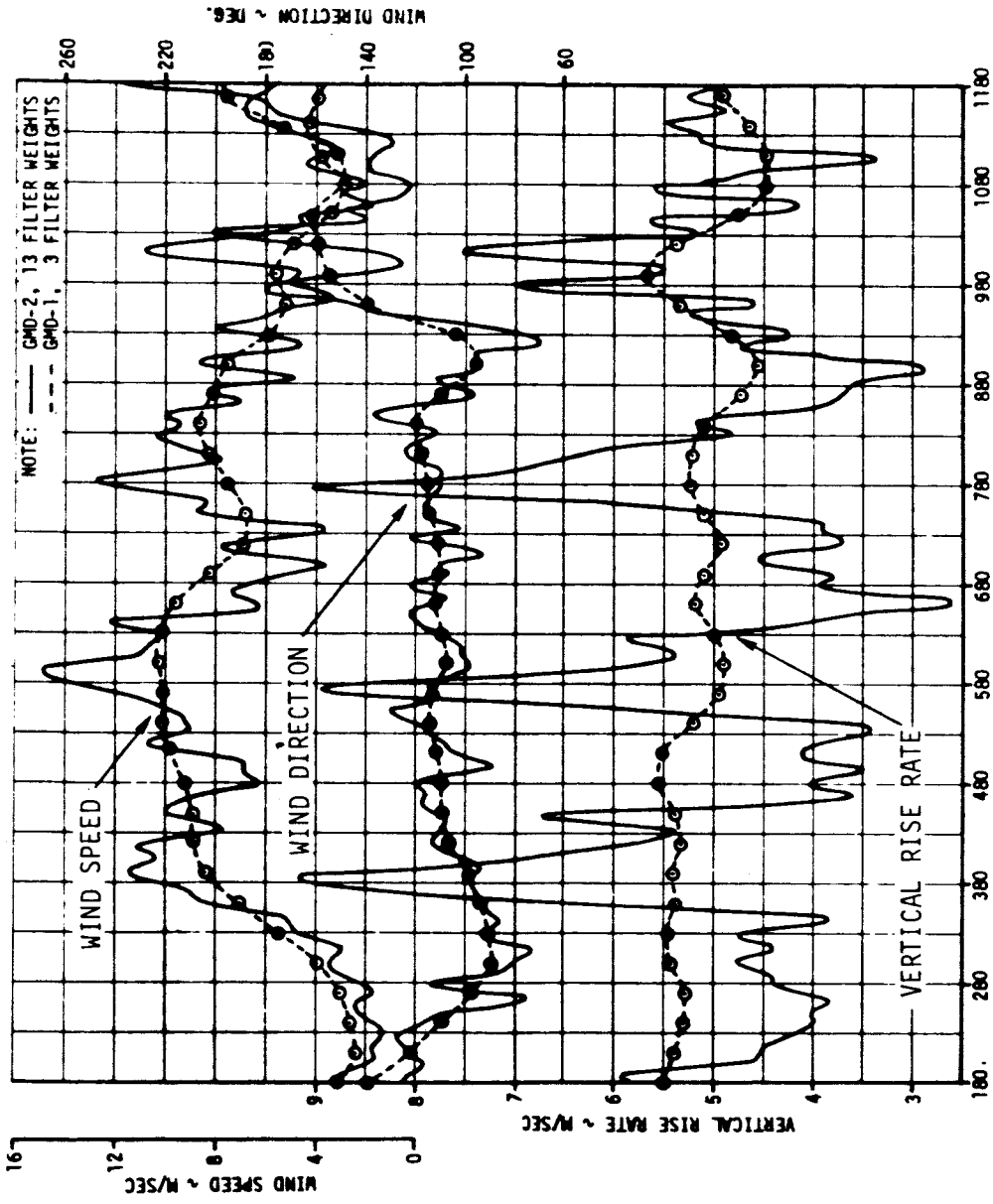

FIGURE 4-3. SIMULTANEOUSLY DETERMINED WINDS - SMOOTHED SPEED, DIRECTION, AND VERTICAL RISE RATES - 1754 GMT, SEPTEMBER 6, 1967 - GMD-1 AND GMD-2 DATA

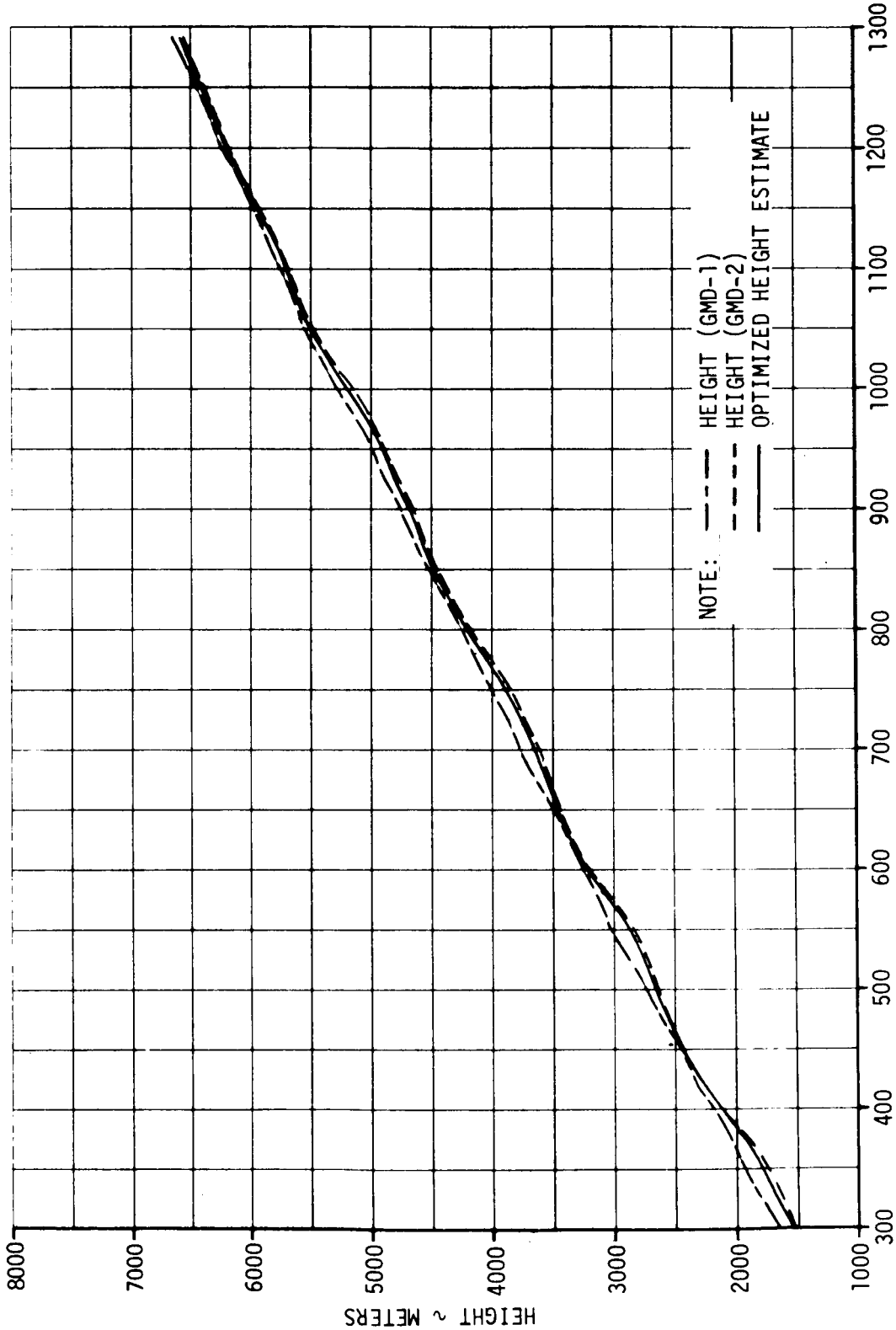

FIGURE 4-4. COMPARISON OF COMPUTATIONS OF HEIGHT AS MADE FROM SIMULTANEOUS GMD-1 AND GMD-2 DATA (1754 GMT, SEPTEMBER 6, 1967) PLUS THE OPTIMIZED HEIGHT ESTIMATE USING THE SAME SIMULTANEOUS DATA

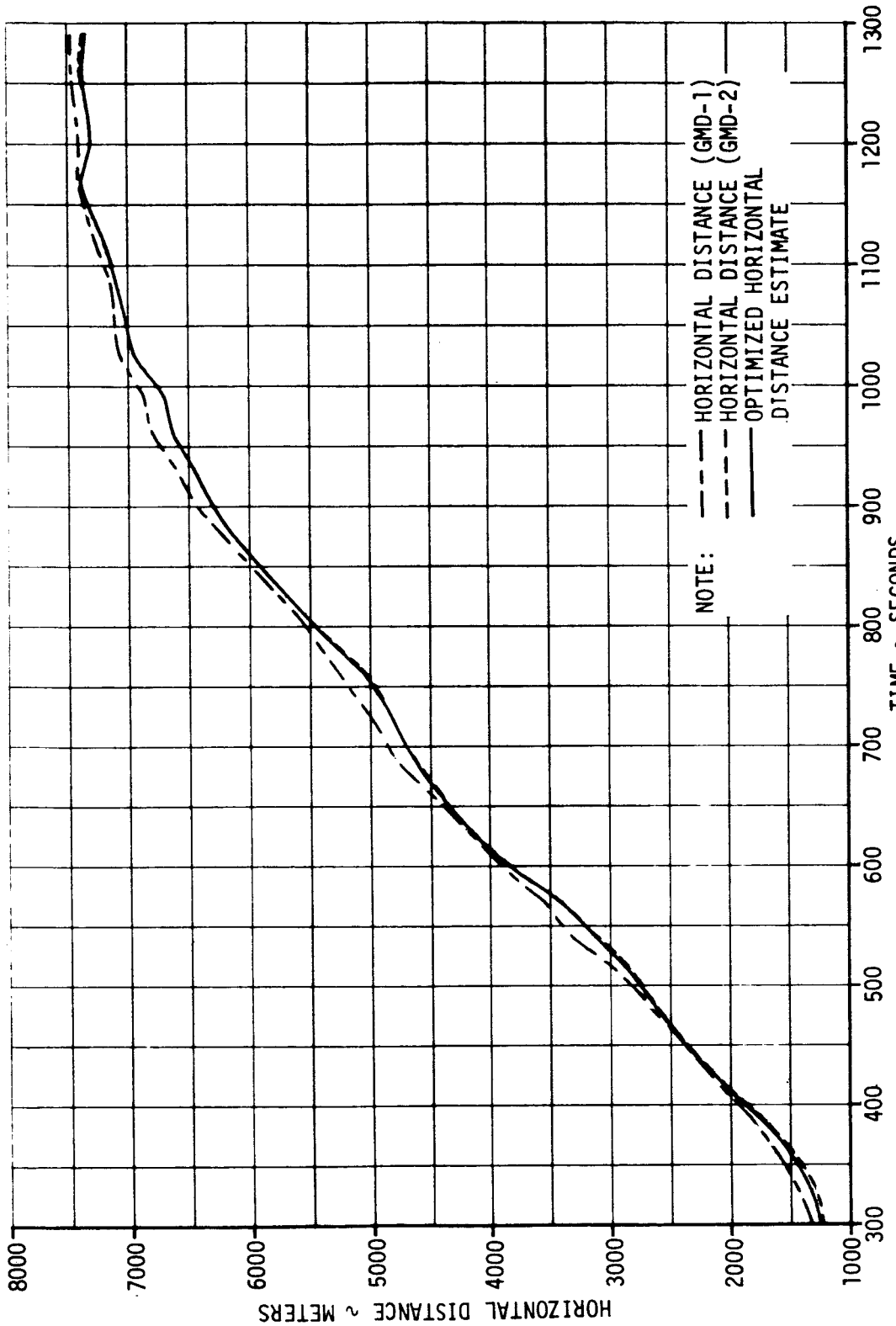

FIGURE 4-5. COMPARISON OF COMPUTATIONS OF HORIZONTAL DISTANCE AS MADE FROM SIMULTANEOUS GMD-1 AND GMD-2 DATA (1754 GMT, SEPTEMBER 6, 1967) PLUS THE OPTIMIZED HORIZONTAL DISTANCE ESTIMATE USING THE SAME SIMULTANEOUS DATA

4.1 (CONTINUED)

The GMD-1 control recorder prints the elevation and azimuth angles to the nearest hundredth of a degree, but the data cards are punched to record these angles only to the nearest tenth. To reduce the truncation error introduced by this procedure, it is recommended that elevation and azimuth angles for the GMD-1 data be punched to the nearest hundredth degree as is done for GMD-2 data.

In GMD-2 data recorded at five second intervals, it is observed that the same temperatures and humidity ordinates are recorded for two or three data cards successively before a change in these values is indicated. The reason for this is in the speed of rotation of the clock-driven commutator on the radiosonde instrument which provides an updated temperature sample only once in an 8.6, a 10.7, and another 10.7-second interval each 30 seconds, and an updated humidity sample once in a 15.4 and a 10.7-second interval. Therefore, the repetition of temperature and humidity ordinates on more than one punched card is because the given data by the ADP still represents the latest information available. The resulting step like lapse rates of temperature and humidity are misleading and introduce some error in the true representation of the pressure profile and the thermal structure of the atmosphere. To eliminate this characteristic of GMD-2 data and also to make its information more compatible with GMD-1, it is recommended that the sampling frequency be reduced to one sample per 15 seconds. This would also tend to filter random noise frequencies from the frequency content of the data and possibly obviate the application of any smoothing filter.

The 200-second cycle appearing in the GMD-2 winds shown in Figure 4-2 was observed in a run of simultaneous data taken on September 6, 1967, at 1754 hours GMT. The frequency of occurrence of such a phenomenon is unknown. It is recommended that a study be made of this phenomenon to determine its cause and source. If such a study showed that this phenomenon occurs occasionally from some characteristic of the circuitry in radar type range measurements, there would be wide sweeping implications with respect to independently observed cyclic changes in rate of rise of balloons in data from other sources.

ADDENDUM TO NASA CONTRACTOR REPORT

NASA CR-61192

January 1968

REVIEW OF RAWINSONDE REDUCTION METHODS

By

R. S. Wheeler, The Boeing Company

RE: Section 4, "Conclusions and Recommendations," (see Figures 4-2 and 4-3) pp. 4-1 through 4-8

The cyclic variation in the winds depicted in Figures 4-2 and 4-3 of CR 61192 has now been investigated. This error was caused by a problem with the NASA Atmospheric Research Facility's AN/GMD-2A Rawinsonde System, specifically, the comparator, which provides the range measurements. A difficulty in the electromechanical linkage induced a cyclic variation in its turning rate. The periodicity of this variation was shown to be approximately three minutes per cycle, the same as that observed in the reduced GMD-2A winds and balloon rise rates. The problem has now been corrected.

When the AN/GMD-2A equipment at the Mississippi Test Facility was checked, it worked perfectly with no cyclic error present. Apparently, the fault is not common to all GMD-2 sets. It is believed that a bent drive shaft, or other cause of binding, is responsible in those sets which produce these variations.

APPENDIX A

ERROR STUDY

1.0 GENERAL

Simultaneous rawinsonde runs of GMD-1 and GMD-2 were studied to provide an insight into the errors entering the recording and reduction of data. One AMQ-9 and one AMT-4 rawinsondes were suspended from a single balloon and tracked by two separate tracking antennae. The antennae are situated approximately 61 meters apart along a near NE-SW base line. Antenna #1, the NE one, is considered the origin of the rectilinear coordinate system for balloon positions. Therefore, to correct the positions determined from Antenna #2 to the origin -41.8 meters is added to Y (W-E) coordinate, -44.5 meters is added to Z (S-N) and 1.1 meters is added to X (Height) for comparison of positions determined from Antenna #1.

1.1 ERROR SOURCES

These site corrections are very much smaller than the differences observed in the balloon positions as reduced from each antenna's range, elevation and azimuth which are generally larger by an order of magnitude. There are a number of factors contributing to these large differences, part of them due to the separate antennae and tracking systems, and part due to basic differences between the methods of determining coordinates.

The separate antennae have identical pedestals, drives, and gears; however, orientation and leveling to the precision required to have the indicated lines of sight meet at the balloon and flight instruments is apparently impossible. The time factor is used as the identifier for simultaneous data; however, each system records its data on the signal from its own timer. That these are not coordinated is evidenced when the azimuth angle is changing rapidly. In one instance when azimuth was changing at a rate of more than one and a half degrees per second, the azimuth lines from the two antennae diverged at an angle of greater than 10 degrees between them at a "simultaneous" reading. At the horizontal-distance-out of the balloon, the azimuths should have converged at an angular difference of from three to five degrees. This would indicate that there could have been as much as a ten second difference between the timers. Because of these obvious differences in the timers, good estimates of bias in leveling and orienting of the two antennae are practically impossible. Examination of the data indicates that the differences are at least 0.3 degree and most probably of the order of 0.5 degree in both elevation and azimuth angles, not from true north or true horizontal but from each other.

In a single rawinsonde run, the timing is not an error factor in the balloon coordinates computation. If, however, timing of the intervals is erratic or is fast or slow, wind speed errors will result which are impossible to detect.

1.1 (CONTINUED)

In addition to the contributions to bias discussed, a very basic difference between the GMD-1 and the GMD-2 systems accounts for a great deal of difference in the determined balloon coordinates. Whereas the GMD-2 directly measures all the components such as range, elevation, and azimuth necessary to determine the rectilinear coordinates of the balloon's position; all of these coordinates in the GMD-1 system are functions of the balloon height which is determined from the reduction of the hydrostatic equation and the pressure data for each data point. This means that the balloon height and indeed the horizontal coordinates are functions of the pressure, temperature, and humidity, each subject to error in measurement. GMD-1 coordinates are also functions of the azimuth and elevation angles and their errors measured by the tracking antenna.

1.2 RANDOM ERROR VARIANCE

The sources of error discussed thus far contribute in general to bias differences between the two systems. In addition to these, there are random errors due to noise in the data. An effort to evaluate this contribution to total error was accomplished.

A moving average smoothing filter was applied to the raw data from both GMD-1 and GMD-2 systems, and the residuals determined by subtracting from each raw data point its respective smoothed value. The transfer functions of two of these filters are shown in Figure A-1. The sum of the squared residuals was then divided by the number of data points contributing to each summation to give the mean squares or variance.

With GMD-2 data at a sampling frequency of 0.2 samples per second this method does give some insight into the true variance of the data. The smoothing filter employed has a cutoff frequency such that wave lengths longer than about 400 meters were passed and all wave lengths shorter than about 125 meters were filtered into the residuals. The wave lengths between were partially passed and partially filtered in the roll-off interval of the filter's response.

Valid wind variations that can be measured by the rawinsonde systems and to which the balloon can respond should include only wave lengths greater than about 150 meters. Higher frequency variability must be credited to the "noise" in the data. The sampling rate of GMD-1 does not really permit filtering since the shortest wave length it can sense is about 300 meters. Although GMD-1 data were filtered with the same filter used on GMD-2 data, the effective separation is between wave lengths greater than 2500 meters from wave lengths of between 300 and 750 meters. Higher frequencies not due to real wind variation are entirely eliminated. Hence, all variance thus determined is due to the variability of the wind structure and is not because of "noise" in the data.

In reviewing the literature (References 7, 8, 18, and 19), one finds generally quoting the manufacturer, claims of standard deviations of 25 meters in slant range, 0.1 degree or less in elevation and azimuth angles and

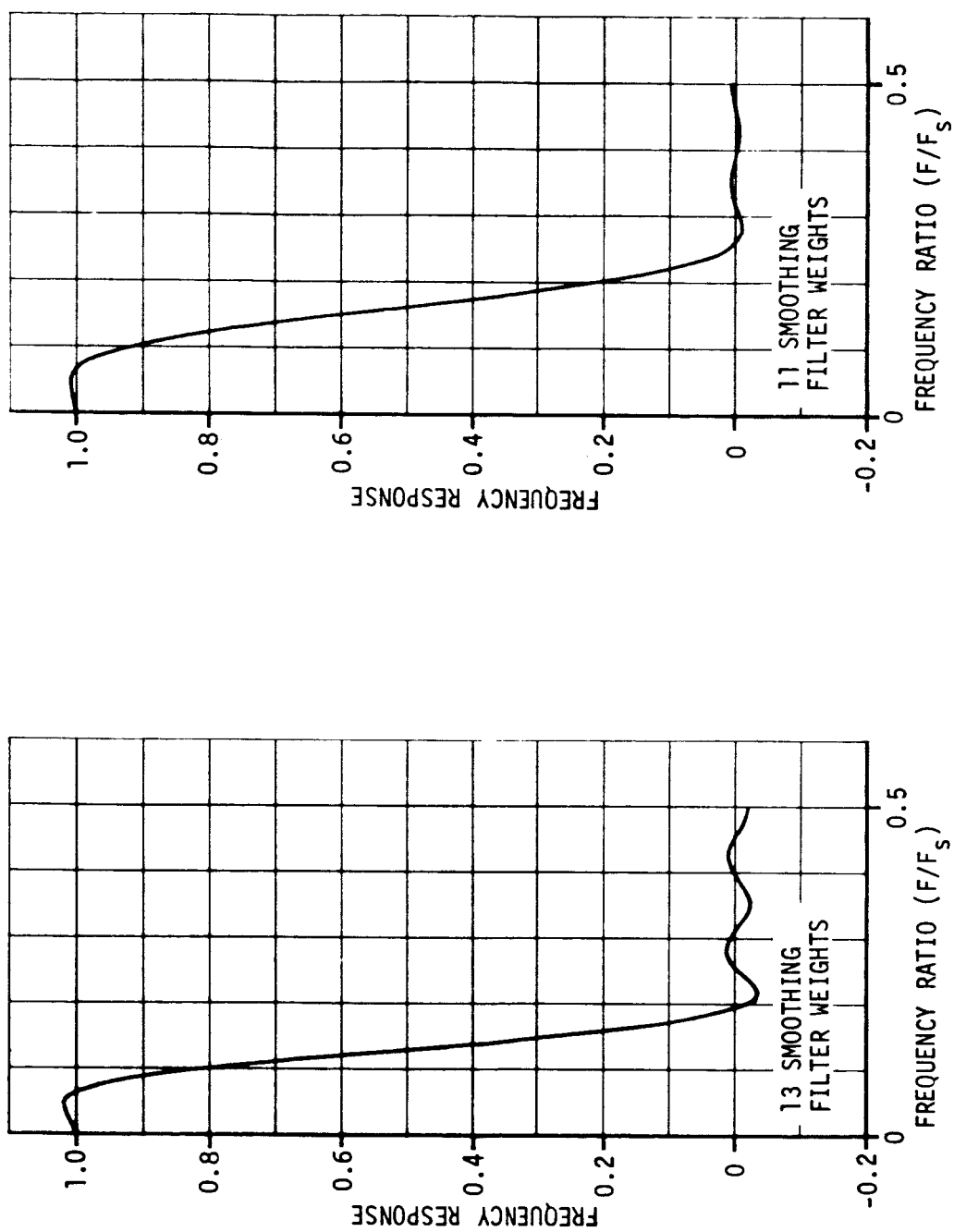

FIGURE A-1. TRANSFER FUNCTIONS OF MARTIN SMOOTHING FILTERS ADOPTED FOR DETERMINATION OF VARIANCE IN MEASURED AND COMPUTED COORDINATES

1.2 (CONTINUED)

2 percent in height. An USAF Air Weather Service Study (Reference 9) gives as results, a 1 percent error in height at 3 Km increasing to greater than 3 percent at 30 Km which is in general agreement with the 2 percent relative error.

In the variance determination from the study of GMD-2 data, the random errors in slant range appear to be less than the claim of 25 meters standard deviation and to be of the order of 10 meters. However, the limited number of cases used in the variance determination leaves the 25 meters standard error as probably the more realistic value. In elevation and azimuth angles the variance study gave approximately 0.1 degree standard deviation in agreement with the accuracies claimed by the manufacturers. The argument that the variance study covered too few cases may hold for the angle measurements as well as slant range in which case the standard errors in azimuth and elevation may be significantly greater than the quoted 0.1 degree.

For height errors, the variance study had to employ GMD-1 data so that the results are probably not significant because of the low sampling rate. The results were considerably less than the relative errors quoted above but did approximately agree with the value used by H. M. de Jong (Reference 8) of 20 meters as the random standard error inherent in the random fluctuations of the sensors.

1.3 OPTIMIZATION OF COORDINATES

The major benefit of the simultaneous runs of GMD-1 and GMD-2 with their respective flight equipments attached to a single balloon is in the opportunity to apply estimation theory to this "overdetermined" system and compute optimized estimates of the balloon's coordinates including calculations of the minimized variance at each data point. Using the elevation and azimuth angles and the slant range from the GMD-2 data and the independent heights calculated from the GMD-1 pressure, temperature, and humidity data; the estimations of the optimum heights and distances out from the antenna were computed using the procedures set forth by de Jong (Reference 8). The variances of slant range, azimuth elevation angles, and height are required inputs to the calculations. Various values for these were tried to assess the effect on the results.

Further effort to optimize the estimate of the balloon position was attempted in computing the HDO by employing the azimuths of both antennae to triangulate the position. The increase in dimensions entails an increase in the size of the covariance and Jacobian matrices and the complexity of the matrix operations required in the application of estimation theory to optimize the results. That there is no really significant improvement (see Figure A-2) over the "two-dimensional" approach of de Jong's (Reference 8), is mute testimony to the rule that the number of basic calculations should not exceed M+1, where M is the number of constraints imposed.

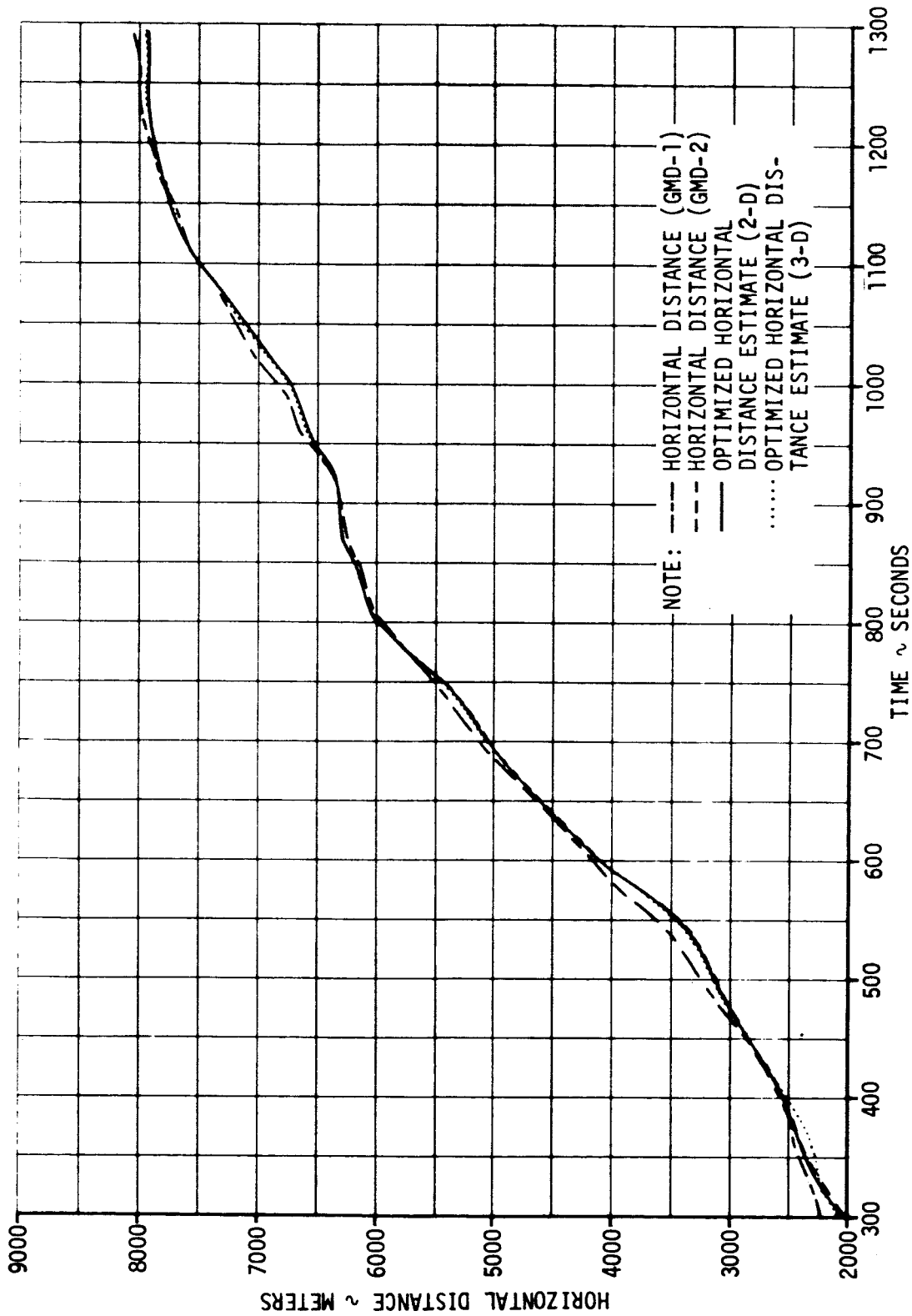

FIGURE A-2. COMPARISON OF COMPUTATIONS OF HORIZONTAL DISTANCE AS MADE FROM SIMULTANEOUS GMD-1 AND GMD-2 DATA (1420 GMT, SEPTEMBER 6, 1967) PLUS A 2-DIMENSIONAL AND A 3-DIMENSIONAL OPTIMIZED HORIZONTAL ESTIMATE USING THE SAME SIMULTANEOUS DATA

1.3 (CONTINUED)

In general, the results appear to be sensitive to the values used. The minimized variance of the distance-out of the balloon is sensitive to the values used as angle variances while the minimized variance of the height is sensitive to the values used for slant range and height as would be anticipated.

Linear estimation theory is of interest only in determining the degree to which variance in reduction of balloon coordinates can be minimized. The simultaneous runs made with the AMQ-9 and the AMT-4 radiosondes attached to a single balloon permit application of linear estimation theory at the cost of considerable effort and the expense of the extra radiosondes. The improvement in the determination of height and horizontal coordinates of the balloon is not considerable. For this reason, this procedure is not recommended. If however the AMQ-9 provided a telemetered pressure measurement in addition to slant range measurement, linear estimation techniques could be applied to the reduction methods resulting in some improvement in accuracy of the winds determined as well as improved accuracy for the pressure-height profile. Examples of the degree of improvement by application of estimation theory are shown in Figures 4-4, 4-5 and A-2. As indicated however, it is important to use realistic and as accurate as possible values of the variance in measurement of slant range, elevation and azimuth angles, and computation of balloon height from pressure measurement. It can be seen in Figures 4-4 and 4-5 that by underestimating the true variance value of slant range, the optimized values of both height and HDO, and the plots of the calculated estimation, give too much credence to the straight GMD-2 calculations of these coordinates. Particularly in the plots of height with time the GMD-1 results appear to be more credible since they fall on a fairly straight line with a more or less uniform slope.

APPENDIX B

REDUCTION OF THERMODYNAMIC PROPERTIES

1.0 GENERAL

The formulae and procedures reviewed in this appendix are only those for which alternatives are given. Also if other formulae such as for humidity do not pertain to the type of sensing element used at MSFC, they will not be included in this review.

1.1 PROPERTIES

1.1.1 Temperature

a. The strict proportionality maintained by the radiosonde transmitter between two audio frequencies and two resistances in the circuit (Reference 7) is exploited in reducing temperature from the AN/TMQ-5 recorder divisions on the strip chart. The TMQ-5 is, in fact, a recording frequency meter and the divisions or ordinates are a measure of the audio frequency modulation of the carrier signal. Twice the number of ordinates counted from the left margin of the strip chart equals the frequency of the modulation (or more properly, the frequency of the transmitter's blocking oscillator), and this frequency is the function of the resistance of the temperature sensing element. With these relationships, the temperature, t, may then be derived as a function of the ratio of the resistance of the element at the measured temperature during the preflight calibration procedure known as the baseline check. The resistance of the element at the baseline temperature is given in the literature (References 10 and 11) by the empirical formula:

$$R_c = \frac{2.137 \times 10^7}{2\, d_b} - 1.125 \times 10^5 \qquad (B.1)$$

where d_b is the baseline temperature ordinate. The resistance of the element at the temperature, t, is given by the similar formula:

$$R_t = \frac{2.137 \times 10^7}{2\, d_t} - 1.125 \times 10^5 \qquad (B.2)$$

where d_t is the ordinate observed at temperature t. The validity of the empirical constants employed in the above two equations is dependent on the resistance of the temperature element meeting the rigid specifications to which it is manufactured. The specifications require that at a temperature of 30°C, the element must have a resistance of 40,000 ohms. The relationship between this resistance, R_{30}, and that at the baseline temperature is given in the literature as follows:

1.1.1 (Continued)

$$\log_{10} R_{30} = \log_{10} R_c + 5.26316 \log_{10} [0.005(t_b+170)] \quad (B.3)$$

where t_b is the temperature of the baseline check in degrees Celsius. Simplifying, we get:

$$R_{30} = R_c [0.005(t_b + 170)]^{5.26316}$$

or,

$$0.005(t_b = 170) = \frac{R_{30}}{R_c}^{\frac{1}{5.26316}} = \frac{R_{30}}{R_c}^{0.19} \quad (B.4)$$

The relationship between the ambient temperature, t, and the ratio of the resistances R_{30} to R_t is given in the literature as follows:

$$\log_{10} (t + 170) = 2.30103 + 0.19(\log_{10} R_{30} - \log_{10} R_t) \quad (B.5)$$

which can be similarly simplified to read:

$$t + 170 = 200 \frac{R_{30}}{R_t}^{0.19} \quad (B.6)$$

From Equation B-4:

$$(R_{30})^{0.19} = (R_c)^{0.19} (t_b + 170)\ 0.005$$

which, if substituted into Equation B-6, makes the formula for temperature in degrees Celsius:

$$t = (t_b + 170) \left(\frac{R_c}{R_t}\right)^{0.19} - 170 \quad (B.7)$$

In this form the equations to derive temperature become a handy and useful tool, and the value of R_{30} does not appear in the reduction formulae.

b. In Reference 12, values of the empirical constants used in Equation B.1 and B-2 were given as 21710 in place of 2.137×10^7 and 114.2 in place of 1.125×10^5. These were used and compared with the results using the constants given in Equations B-1 and B-2. Results were within about a tenth of a degree at all data points. Selection of the constants then was based on which of the two sets gave the closer value to the calibration temperature from the CP-223A/UM calculator for the calibration ordinate of 37.6. For this reason, the values given in Equations B-1 and B-2 and quoted in References 10 and 11 are the recommended values.

1.1.1 (Continued)

c. The reduction formulae for temperature currently used at the MSFC Atmospheric Research Station is the most frequently mentioned in the literature (References 3, 4, 13, and 14) on computer reduction of rawinsonde data. It is based on the calibration temperature, t_c, corresponding to 37.6 recorder divisions from the CP-223A/UM calculator after setting up the baseline check relationship. The formula for temperature in degrees Centigrade is:

$$t = \left(\left|\frac{d_t - 37.6}{b}\right|\right)^a \left(\frac{t_c + 20.525}{2.2625} + 64\right) + t_c \qquad (B.8)$$

where d_t is the temperature recorder division value, and t_c, in degrees Celsius, is usually within one degree of -19°C. Different empirical constants in the evaluation of a and b are used depending on whether the term $(d_t - 37.6)$ is positive or negative. If $(d_t - 37.6)$ is positive:

$$b = 39.4$$

$$a = 1.177 + \frac{1}{2}\left[\frac{d_t - 37.6}{b}\right]^2$$

and when $(d_t - 37.6)$ is negative, the first term of the right side of Equation B-8 is multiplied by (-1) and:

$$b = 34.6$$

and

$$a = 1.24 + 1.06383\left[\frac{d_t - 37.6}{b}\right]^2$$

As can be readily seen, the value of t converges on t_c as $(d_t - 37.6) \quad 0$.

d. With the same data being run through both temperature reduction methods, results were obtained and compared. Figure B-1 shows extracted portions of the two temperature curves to demonstrate their behavior in the vicinity of t_c, the calibration temperature for 37.6 ordinates. Although the 37.6th ordinate value was passed in the time interval between data points, the curve representing the resistance ratio method appears to pass through the value of t_c almost exactly, and it does so without any discontinuity or significant change in the slope. The dashed curve representing temperatures derived by the second and more commonly used method must inherently pass through the value of t_c at the ordinate value of 37.6; but, as is well demonstrated, it does so by means of an inflection point and considerable change in the slope. The two

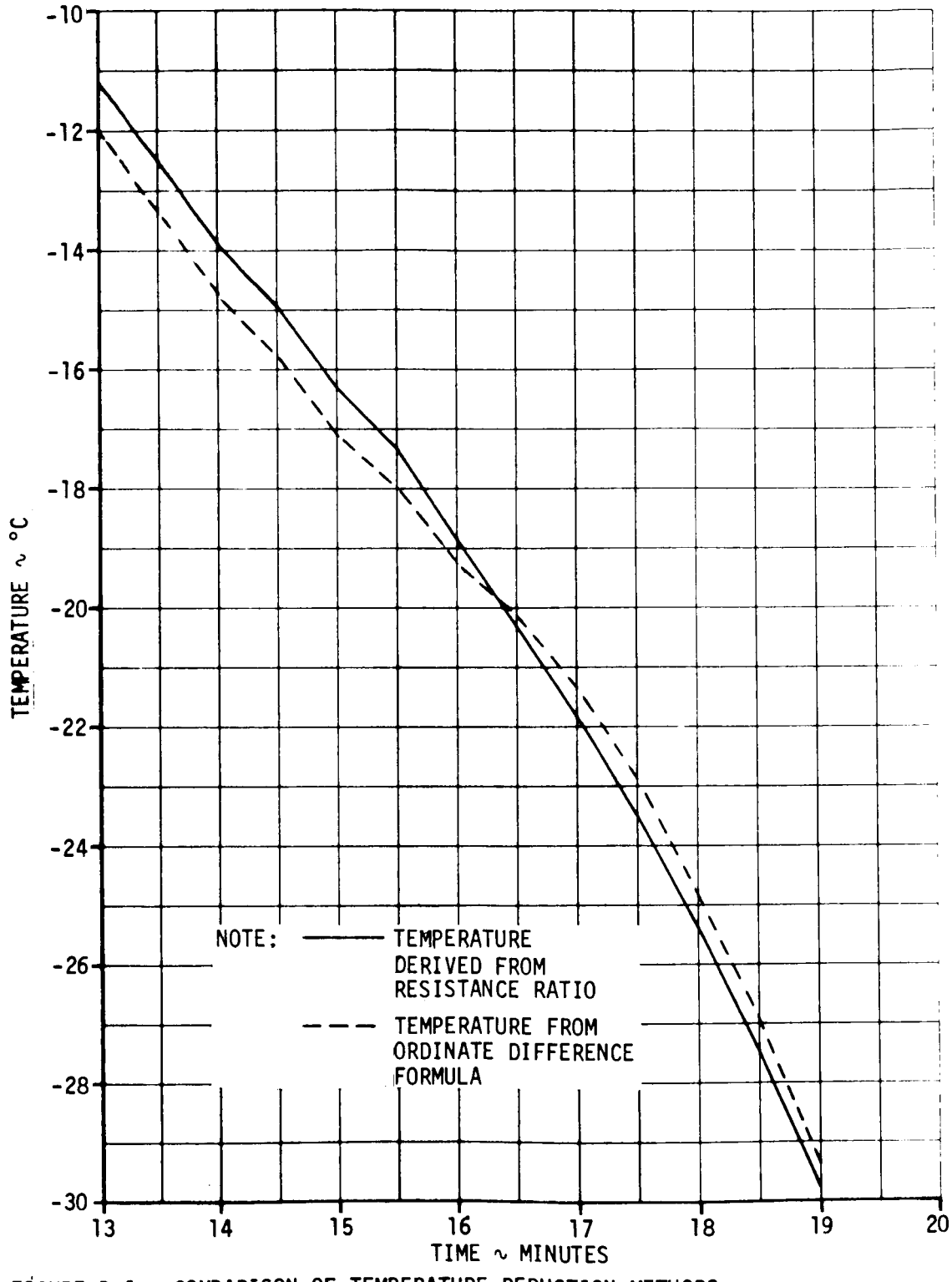

FIGURE B-1. COMPARISON OF TEMPERATURE REDUCTION METHODS

1.1.1 (Continued)

curves tend to converge at both ends of the run, but the behavior of the dashed curve at the calibration temperature leads to the conclusion that the temperatures derived from the resistance ratio formulae are more accurate and more representative of the actual temperature profile of the atmosphere. Hence, the resistance ratio method is recommended.

1.1.2 Relative Humidity

A review of the literature (References 3, 4, 10, 11, 12, 13, and 14) shows a number of reduction techniques for evaluating relative humidity from the recorder division ordinates for humidity. The first of these is the evaluation of a ninth order polynomial whose coefficients are functions of the calibration humidity and ambient temperature and involve combinations of forty given empirical constants. A second reduction formula is an approximation having eleven terms involving functions of the ratio of the resistance corresponding to the humidity ordinate for ambient humidity and temperature to the resistance specified for relative humidity of 33 percent at a specified temperature. Admittedly, this reduction formula is capable of producing both negative values and values greater than 100 percent and would need correcting for such results.

The most commonly used reduction technique for the carbon element (see References 3, 4, 13, and 14) is a method employing two sets of constants, the choice of which depends on whether the term $(46-d_f)$ is negative or positive. d_f is the humidity recorder division ordinate. The relative humidity, U, in percent is determined from the following:

$$U = f_{40} + d_f \left(\frac{f_{40} - 33}{1050} \right) \sqrt{t + 40} \qquad (B.9)$$

At temperatures lower than -40°C, the second term on the right becomes imaginary so a constraint is imposed that this term vanishes when $t \leq -40$. f_{40} the relative humidity corresponding to an ordinate of 46 at a temperature of -40°C is evaluated as follows:

$$f_{40} = f_c + \left(\left| \frac{46 - d_f}{c} \right| \right)^a \quad (b) \qquad (B.10)$$

where f_c is the calibration relative humidity.

When $46 - d_f > 0$

$$a = 1.66 + \frac{46 - d_f}{33}$$

$$b = 100 - f_c$$

1.1.2 (Continued)

$$c = 64.8 - \frac{f_c}{2.51}$$

and when $46 - d_f < 0$

$$a = 0.5 - \left(\frac{46 - d_f}{10}\right)$$

$$b = 10 - f_c$$

$$c = \frac{f_c}{1.45} - 5.198$$

Despite the complexity of this method of humidity reduction, it is simpler than the ninth order polynomial mentioned first among the reduction methods for programming. The formula given by Equation B.9 may be less accurate, but the inaccuracy of the sensor is sufficiently large that the inaccuracy of the reduction method is relatively insignificant.

The reduction method associated with Equation B.9 is selected for use by MSFC. In this recommendation, acknowledgement is made of the fact that this is the currently used technique and reprogramming is hardly worthwhile.

1.1.3 Virtual Temperature

There are three formulae in more or less common use for the derivation of virtual temperature. In the main, these are derivable from the equation of state, Dalton's Law, and the ratio of the molecular weight of water vapor to the equivalent molecular weight of dry air. They are: (for virtual temperature in degrees Kelvin)

$$T^* = T \frac{P}{(P - 0.37812e)} \tag{B.11}$$

$$T^* = T \left(\frac{P + 0.00123e}{P - 0.37812e}\right) \tag{B.12}$$

and,

$$T^* = T \left(1 + 0.376432 \frac{e}{P}\right) \tag{B.13}$$

or

$$T^* = T \left(\frac{P + 0.376932e}{P}\right)$$

1.1.4 Horizontal Distance Out (HDO) and Curvilinear Coordinates

a. Elevation and azimuth angle coordinates of the balloon from the antenna are measured directly from either the GMD-1 or GMD-2 systems. With the additional direct measurement of slant range, all the data necessary for the determination of the winds is available for the GMD-2 system. For the GMD-1 system, however, the slant range can be determined by means of the following equation for slant range (see Reference 3):

$$R = [(R_E+H+X')^2 - (R_E+H)^2\cos^2 E]^{1/2} - (R_E+H)\sin E \qquad (B.14)$$

The balloon position in an orthogonal curvilinear coordinate system can be determined with these data for each time data point; and differentiation with respect to time gives the magnitude of the wind components.

b. An alternate coordinate to determine slant range for GMD-1 winds is to calculate the plan-view distance of the balloon from the antenna on the tangent plane through the antenna. This distance, normally called the Horizontal-Distance-Out (HDO), can be calculated directly without first computing slant range. The formula is:

$$HDO = (R_E+H+X')\cos\left[E+\sin^{-1}\frac{(R_E+H)\cos E}{R_E+H+X'}\right] \qquad (B.15)$$

When slant range is measured directly as with GMD-2 the formula then is simply:

$$HDO = R\cos E$$

In either case HDO should be determined to compute the curvilinear coordinates of the balloon position. All these formulae are exact and can be derived each from the other. Hence, if there were no truncation errors involved, the results for HDO, X, or R would be the same without regard to which formula was used to determine them. Even with truncation on the squares of very large numbers, e.g., R_E in meters or on irrational numbers, the effect is usually less than five parts per million on computer results. Nevertheless, it is recommended that for further reduction of the balloon positions in rectilinear coordinates the HDO be computed directly for GMD-1 data because it minimizes truncation errors introduced by the computer and because HDO must be determined anyway.

1.1.4 (Continued)

c. An alternative to computing HDO for deriving the curvilinear coordinate Y and Z is presented in Reference 6. This alternative introduces the parameter, F, which is evaluated in terms of the radius of the earth, the height of the antenna above sea level, the height of balloon above the reference sphere, and the slant range of the balloon from the antenna:

$$F = \frac{(R_E+H)^2 + (R_E+H+X')^2 - R^2}{2(R_E+H)\ (R_E+H+X')} \qquad (B.16)$$

With reference to Figure 2-1 and a little manipulation, it is readily seen that identically:

$$F \equiv \text{Cos } \theta$$

where θ is the internal angle at the earth's center whose arc on the surface of the reference sphere is equivalent of the balloon's tangential displacement from the antenna.

Because the evaluation of F requires the computation of slant range even when it is not directly measured as with GMD-1 data, use of the F parameter is an unnecessary complication in the reduction of the curvilinear coordinates.

The curvilinear coordinates, Y (positive to the east) and Z (positive to the north), are defined by the following equations:

$$Y = (R_E+H)\ \sin^{-1}\left[\frac{HDO\ \sin A}{R_E+H+X'}\right] \qquad (B.17)$$

and

$$Z = (R_E+H)\ \sin^{-1}\left[\frac{HDO\ \cos A}{R_E+H+X'}\right] \qquad (B.18)$$

where A is the azimuth angle measured by the antenna system. If the F parameter is used, the term $(1 - F^2)^{1/2}$ is substituted within the brackets of Equations B.17 and B.18 for the identically equal term $HDO/(R_E+H+X')$.

1.1.4 (Continued)

where T is temperature of the atmosphere in degrees Kelvin

e is the partial pressure in mb due to water vapor

and P is the total pressure of the moist atmosphere.

The similarity in the three formulae is immediately apparent and the use of any one of them in the range of atmospheric pressures, temperatures, and humidities makes differences of the order of .01 degrees in the resulting values of virtual temperature. Although these differences are small, the effect of a bias error in virtual temperature is cummulative in the determination of balloon height from GMD-1 or in the determination of pressure from GMD-2 data. However, the accumulated error introduced in height is of the order of one meter or less for the summation of thicknesses from the surface to 20,000 meters.

The first Equation, B.11, is a development of the equation of state for the total density of the moist air, and the coefficient is derived in calculating as precisely as possible the difference between unity and the ratio of the molecular weight for water vapor to that for dry air (Reference 2). In this equation, the water vapor is treated as an ideal gas which is only an approximation. However, throughout the range of meteorological conditions, the contribution to error by this approximation is less than a tenth of one percent and decreases rapidly with decreasing temperature (Reference 15).

The formula given in Equation B.12 (References 3 and 4) appears to have been derived in applying a fixed correction value to compensate for the fact that water vapor does not behave as an ideal gas. The references do not give the source for, nor an explanation of, the constant coefficient used as the correction factor. If as assumed, the additive used as a coefficient for vapor pressure is a correction factor, its validity is good for a humid atmosphere only in a range of temperatures close to 20°C. At lower temperatures, the formula should revert back to that given in B.11.

Equation B.13 presents a formula which, though similar to B.11 and B.12, uses a coefficient for vapor pressure whose derivation is completely obscure. References 11, 13 and 14, presenting this formula to determine T*, give no source nor explanation of the constant used. To be equivalent in value of T* derived from B.11, the coefficient of e should be approximately 0.3796; and to approximate the values of T* computed by B.12, the coefficient would have to be still larger in value.

Since the equation for virtual temperature determined by B.11 produces values of T* in the range of the "golden mean" between the values computed by the other two formulae, it is recommended that virtual temperature be determined by the formula of Equation B.11.

APPENDIX C

WIND REDUCTION PROCEDURES AND DIGITAL FILTERS

1.0 WIND REDUCTION PROCEDURES

In this study, three separate techniques (see Figure C-1) were tried in the wind reduction to provide smoothed values of the wind. The first of these techniques named MOD-1 is a straightforward coordinate transformation from given range (or HDO), azimuth, and elevation data. A differentiating filter is then applied to determine the wind components and to smooth their values in one operation.

The other two techniques both apply smoothing to the raw data before any coordinate transformations are performed. One of these (MOD-2) then applies the differentiation to smoothed range, azimuth, and elevation which are then transformed directly to wind components without any computation of rectilinear coordinates. The third method (MOD-3) applies smoothing to raw data of range, azimuth, and elevation after which rectilinear balloon coordinates are determined, and then straightforward differentiation of balloon positions with respect to time gives the wind components.

MOD-3 is the procedure currently used by MSFC in determining winds. The MOD-2 method was originally designed to test the concept that by applying a combined smoothing and differentiating filter to the R, E, and A data first, all random uncorrelated errors could be eliminated prior to combining them through the transform operation of determining the orthogonal coordinates. This concept, despite its intent, does not work because the equations to transform the time derivatives $\dot{R}$, $\dot{A}$, and $\dot{E}$ into $\dot{X}$, $\dot{Y}$, and $\dot{Z}$ are not free of the undifferentiated values of R, A, and E. Therefore, as can be seen in the flow chart diagram of MOD-2, a smoothing filter must be applied to R, A, and E prior to differentiation. As a result, the winds determined by this procedure are almost exactly the same as those derived by MOD-3. Figures 4-2 and 4-3 are plots of winds derived from the same rawinsonde data and the curves for either GMD-1 or GMD-2 data represent the results from either MOD-2 or MOD-3 wind reduction procedures.

The results from MOD-1 are close to results indicated for MOD-2 and MOD-3 except that the peaks and troughs are slightly sharper and their amplitudes slightly greater, particularly for GMD-2 winds. MOD-1 results for GMD-1 show more random scatter of the wind data points demonstrating the mistake of combining the individual errors in the raw data through transforming the coordinates before any smoothing process is applied.

Because MOD-2 provides no significant improvement or difference in the winds from those of MOD-3, and because MOD-2 is a considerably more complex programming problem, MOD-3 is the recommended procedure for wind reduction.

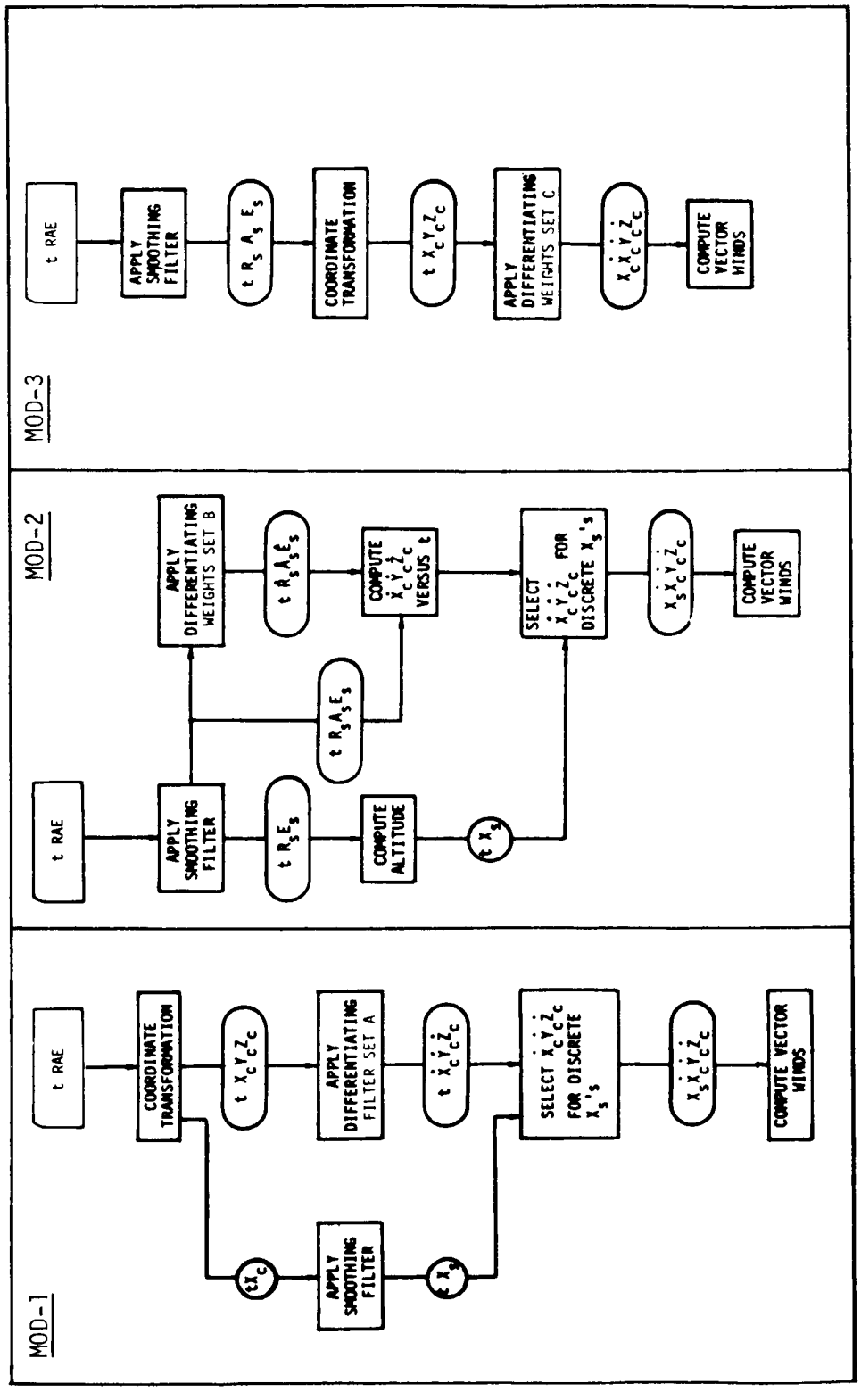

FIGURE C-1. LOGIC AND DATA FLOW CHARTS FOR WIND REDUCTION PROCEDURES. (SUBSCRIPTS S AND C REFER TO SMOOTHED AND CURVILINEAR, RESPECTIVELY. DOTTED COORDINATES ARE DERIVATIVES WITH RESPECT TO TIME; HENCE, THEY ARE THE RESPECTIVE WIND COMPONENTS

1.1 DIGITAL FILTERS

Much has been written on digital filters for both smoothing and differentiating (References 6, 16 and 17). The various types of filters are well discussed and their individual advantages and disadvantages enumerated. With the assumption that the true measurement of the wind and the error components are band-limited to disjoint frequency bands, smoothing and differentiating digital filters derived from Fourier integral theory are optimum. The Martin filters based on a sine rolloff between the cutoff and termination frequencies are the best of these and the most efficient in giving a specified accuracy with the fewest number of weights.

Filters whose weights are proportional to the ordinates of the normal curve or to binomial coefficients have transfer functions that show modification of all frequencies in the domain since the cutoff frequency is zero. Furthermore, they are smoothing filters only; and because differentiating is required, it should be a distinct advantage to perform smoothing concurrently with differentiating. For this reason, the differentiating type of filter is of great interest. Therefore, the Martin filter with a distinct cutoff frequency other than zero which can be specified is recommended for use with wind reduction techniques.

Designing the correct filter for wind reduction requires knowledge of the statistical properties of the noise or error components to be filtered out of the data. However, such properties of the noise as variance, serial correlation, and distribution are not explicitly known. One must theorize as to the maximum frequencies which are significant of the true wind field and to which the rawinsonde system will respond. This must largely be based on observation and certain limiting factors such as the sampling rate of the rawinsonde. Then, one can easily design the filter to eliminate all higher frequencies.

The sampling rate of the GMD-1 of one sample per 30 seconds limits the highest frequency that can be discerned to one cycle per minute, a wave length of about 300 meters; the spectral power of all shorter wave lengths is folded into the apparent power of lower frequencies. Wave lengths of 300 meters and longer, however, must be considered as "signal" or part of the true wind field. For this reason, it is probably inadvisable to attempt to filter GMD-1 data at all.

1.1 (CONTINUED)

An important question to be answered before designing a digital filter is how much of the data record length can one afford to sacrifice. The total number of filter weights less one defines the number of data points lost in the numerical filtering process, one half at each end of the record. However, the greater the number of weights used, the sharper is the delineation between passed and filtered frequencies; and it is desirable to have sharp delineation if the limits of disjoint frequencies can be precisely defined. If, however, there are very long wave systematic cyclic phenomena that are inherent characteristics of the measuring sets, such as appears to be the case for the GMD-2 winds depicted in Figures 4-2 and 4-3, it may be desirable to have a long rolloff interval so that those frequencies that are not exclusive to either signal or noise can be at least partially passed. A band pass filter can be designed to handle and filter out a narrow band of frequencies but only at a heavy cost in length of the record; and for even GMD-2 rawinsonde data, this can hardly be afforded.

Figures 4-1, A-1, and C-2 give the response functions of various Martin type smoothing filters which illustrate the capabilities of this filter. Although these plots represent the response of smoothing filters, the weights of differentiating filters are computed from the weights of a particular smoothing set so that the response characteristics are the same as for the smoothing filter from which the differentiating filter was calculated.

The filters whose responses are shown in Figure 4-1 are the filters used for the GMD-1 and GMD-2 wind profiles depicted in Figure 4-2. The filter used for GMD-2 wind data shown in Figure 4-3 is represented by the response shown in C of Figure C-2. No filters were used on the GMD-1 winds.

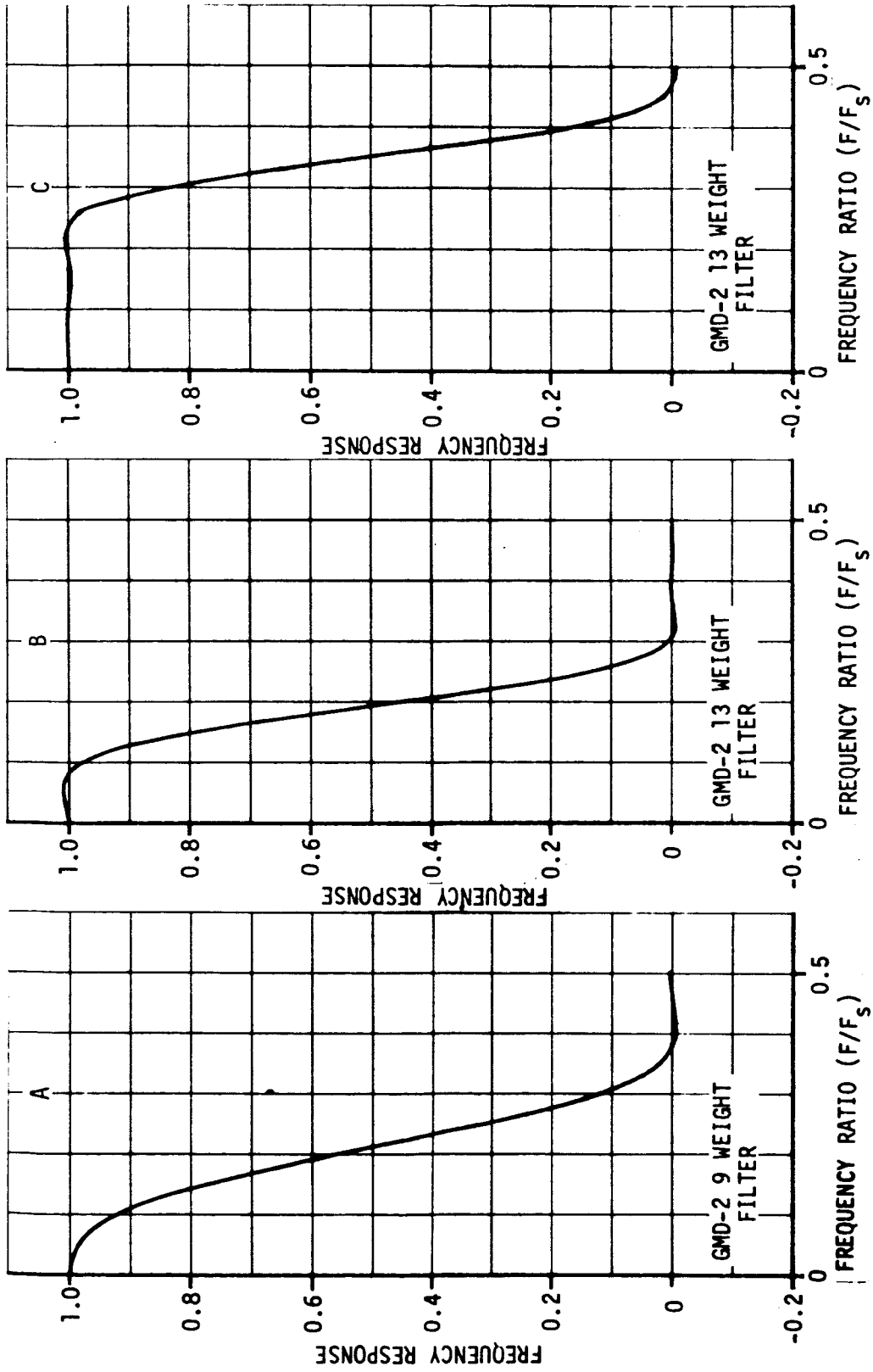

FIGURE C-2. CONSTRAINED MARTIN TYPE SMOOTHING FILTER FREQUENCY RESPONSES

APPENDIX D

LIST OF SYMBOLS

A	Antenna azimuth angle measured clockwise from true north
a	An exponent whose values are computed by given formulae
b	A factor in reduction formulae which is assigned various values
c	A constant in reduction formulae which is assigned various values
C_s	Speed of sound in meters per second
D	The acute angle between the wind axis and the local meridian, arc sin $\lvert\mathring{Y}/\mathring{Z}\rvert$
d_b	Baseline temperature ordinate, to nearest tenth ordinate
d_f	Humidity ordinate, to nearest tenth ordinate
d_t	Temperature ordinate, to nearest tenth ordinate
E	Antenna elevation angle
EXP[]	Base of natural logarithm raised to the power expressed in brackets
e	Vapor pressure, the partial pressure in mb. due to the water vapor content in the atmosphere
F	Parameter used in transforming to curvilinear coordinates
f	Frequency of any cyclic or wave function, cycles per second
f_c	The calibration relative humidity in percent corresponding to 46 ordinates at a temperature of -40°C.
f40	An intermediate relative humidity in percent prior to application of temperature correction
f_s	Sampling rate in number of samples per second
H	The height of the antenna above sea level in meters
HDO	Horizontal distance out of the balloon's position
i	A subscript, index number of any particular data point
N	A dimensionless unit utilized to express index of refraction = $(n-1) \times 10^6$
n	Index of refraction for either visible light or for UHF radio frequencies, a dimensionless ratio expressing a measure of the bending of a ray
P	Pressure of the atmosphere in millibars
P′	Atmospheric pressure in Kg (weight) per square meter
P″	Atmospheric pressure in newtons per square meter

LIST OF SYMBOLS (CONTINUED)

P_a	First approximation of pressure at next higher level in GMD-2 pressure reduction formula
Q	An unspecified quantity having a particular value at a data point in a time or space series of data
R	Slant range distance from balloon to antenna, in meters
R_e	Local radius of the earth at mean sea level
R_c	Resistance of the temperature element at baseline temperature
R_H	Radius of the reference sphere centered at earth's center in meters $R_h = R_e + H$
R_t	Resistance of temperature element at temperature t
R* and r'	Latitude dependent constants used in converting geopotential meters to geometric meters
T	Temperature in degrees Kelvin = t + 273.15
T*	Virtual temperature in degrees Kelvin
$\bar{T}$*	Mean virtual temperature in a layer of atmosphere
t	Temperature in degrees Celsius; also time in seconds since balloon release
t_b	Baseline temperature in degrees Celsius
U	Relative humidity in percent
W_d	Direction from which the wind blows, in degrees clockwise from true north
W_s	Wind speed in meters per second
X or X_c	Vertical coordinate in meters everywhere measured along a radial from center of the earth
X'	Radial height of the balloon above reference sphere in meters
X_s	Smoothed values of X
$\dot{X}$	Time derivative of height coordinate, dx/dt; hence vertical speed of balloon in meters per second
Y or Y_c	Curvilinear distance of balloon to East, measured in meters from meridian through antenna along local latitude parallel on surface of reference
Y_s	Smoothed values of Y
$\dot{Y}$	dy/dt, eastward component of wind in meters per second
Z or Z_c	Curvilinear distance of balloon to north, measured in meters from center of antenna along meridian
Z_s	Smoothed values of Z

LIST OF SYMBOLS (CONTINUED)

$\dot{Z}$	dz/dt, northward component of wind in meters per second
θ	The angle at the center of the earth which is subtended by the arc length of the balloon's displacement measured along the surface of the reference sphere
μ	Coefficient of viscosity in newton seconds per square meter
ρ	Density of the atmosphere in kilograms per cubic meter
ρ'	Density in kilograms (weight) seconds squared per fourth power of meters
ρ''	Density in newtons seconds squared per fourth power of meters
Φ	Geopotential height in geopotential meters which are a variable measure of length and a function of the force of gravity and therefore of latitude and height above sea level

REFERENCES

1. SE 008-001-1, "Project Apollo Coordinate System Standards," Office of Manned Space Flight, National Aeronautics and Space Administration, June, 1965

2. "Dynamic Meteorology," Bernhard Haurwitz, McGraw-Hill Book Company, Inc., New York and London, 1941

3. MTP-AERO-63-6, "Computer Evaluation of Rawinsonde Observations," Bettye Anne Case, Marshall Space Flight Center, National Aeronautics and Space Administration, January, 1963

4. MTP-AERO-62-41, "Computer Evaluation of Rawinsonde Data for Space Vehicle Applications," H. B. Chenoweth and B. A. Busbee, Marshall Space Flight Center, National Aeronautics and Space Administration, May 16, 1962

5. NASA TM X-53139, "A Reference Atmosphere for Patrick AFB, Florida, Annual (1963 Revision)," O. E. Smith and D. K. Weidner, Marshall Space Flight Center, National Aeronautics and Space Administration, September, 1964

6. Boeing Document D5-15564, "Data Reduction Methods - FPS-16 Radar/ Jimsphere," Launch Systems Branch, Space Division, Huntsville, Alabama, October 14, 1966

7. Compendium of Meteorology, "Instruments and Techniques for Meteorological Measurement," Michael Ference Jr., American Meteorological Society, Boston, 1951

8. Journal of Applied Meteorology, "A New Process for the Evaluation of Upper Winds," Volume 5, Number 4, H. M. de Jong, American Meteorological Society, August, 1966

9. AWS Technical Report 105-133, "Accuracies of Radiosonde Data," Headquarters, Air Weather Service, Military Air Transport Service, U. S. Air Force, Washington, September, 1955

10. "IRIG Standards for Range Meterorological Data Reduction, Part I - Rawinsonde," Meteorological Working Group, Inter-Range Instrumentation Group, Range Commanders Council

11. RR-TR-67-10, "Fortran Programs to Compute Rawinsonde Data for Military and Weather Bureau Radiosondes," U. S. Army Missile Command, Redstone Arsenal, Alabama, July, 1967

12. Final Report, Item 6, Contract No. AF19(604)3485, "AN/GMD-2 Data Reduction," Richard P. Gagan, Wolf Research and Development Corporation, Boston, April 30, 1960

REFERENCES (CONTINUED)

13. "Electronic Computer Reduction of Upper Air Data," O. H. Daniel, Major, USAF, Air Force Missile Test Center, Florida (unpublished report)

14. "Digital Computer Reduction of AN/GMD-2 Rawinsonde Data," O. H. Daniel, Pan American World Airways, Guided Missiles Range Division, Patrick Airways, Guided Missiles Range Division, Patrick Air Force Base, Florida, May 10, 1962

15. "Introduction to Theoretical Meteorology," Seymour L. Hess; Holt, Rinehart, and Winston; New York, 1959

16. Boeing Document D5-15278A, "Flight Data Conditioning Processes - Analytical Methods and Functional Procedures," Glen C. McMillen, Launch Systems Branch, Space Division, Huntsville, Alabama, February 1, 1967

17. Technical Information Series No. 57SD340, "Frequency Domain Applications in Data Processing," Marcel A. Martin, General Electric, Missile and Ordnance Systems Department, May, 1957

18. Technical Manual TM-11-6660-206-20, "Rawinsonde Sets AN/GMD-1A and AN/GMD-1B, Headquarters, Department of the Army, Washington, September, 1961

19. Technical Order TO 31M1-2GMD2-3, "Rawinsonde Set AN/GMD-2," Secretary of the Air Force, January 15, 1967

DISTRIBUTION

R-SE, Mr. L. Richard

R-EO, Dr. W. Johnson

R-SSL, Dr. Stuhlinger

R-ASTR
- Dr. Haeussermann
- Mr. Blackstone
- Mr. Hosenthien

R-P&VE
- Dr. W. Lucas
- Mr. R. Hunt
- Mr. N. Showers
- Mr. Stevens
- Mr. J. Moore
- Mr. C. Green
- Mr. G. Kroll

R-COMP
- Dr. H. Hoelzer
- Mr. P. Harness
- Mr. A. Jackson
- Mr. R. Cochran

I-DIR, Col. O'Connor

I-MO, Dr. Speer

MS-IP
MS-IPL (8)

I-MT, Mr. L. Nybo

MS-T, Mr. R. Bland

R-AERO
- Dr. Geissler
- Mr. Jean
- Mr. Hagood
- Mr. Lindberg
- Mr. Ryan
- Mr. Rheinfurth
- Mr. Horn

R-AERO (Cont'd)
- Mr. Turner (5)
- Mr. W. Vaughan (2)
- Mr. Stone
- Mr. Baker
- Mr. McNair
- Mr. Murphree
- Mr. O. Smith
- Mr. Fichtl
- Mr. R. Smith
- Mr. C. Brown
- Mr. Falls
- Mr. Daniels
- Mr. Hill
- Mr. Camp
- Mr. Susko
- Mrs. Alexander
- Mr. Kaufman (20)
- Mr. Reed
- Dr. Heybey
- Mr. Dahm

Dr. Isaac Van der Hoven, ARL
Environ. Meteorology Res. Br.
U. S. Dept of Commerece
Weather Bureau
Washington, D. C. 20235

Dr. Duane A. Haugen, CRHB
Air Force Cambridge Res. Lab.
L. G. Hanscom Field
Bedford, Mass. 01731

Lt. Col. Harold R. Montague (2)
U. S. Air Force Staff Meteorologist
Eastern Test Range
Patrick Air Force Base, Fla. 32925

Dept. of Meteorology
College of Mineral Industries
Pa. State Univ.
University Park, Pa. 16802
Attn: Dr. Hans A. Panofsky
Dr. Blackadar (2)

Commanding Officer
U. S. Army Elec. R&D Activity
White Sands Missile Range, N. M. 88002
Attn: SELWS-ME (Mr. W. Webb)

Pan American World Airways
Div. Meteorologist
Patrick Air Force Base, Fla. 32925

Mr. N. Sissenwine, CREW
Air Force Cambridge Res. Labs.
L. G. Hanscom Field
Bedford, Mass. 01731

Mr. Kenneth Nagler
Spaceflight Meteorology Group
U. S. Dept. of Commerce
Weather Bureau
Washington, D. C. 20235

Dr. H. Newstein
Dept. of Physics
Drexel Inst. of Tech.
32nd and Chestnut Streets
Philadelphia, Pa. 19104

Mr. Roy Endlich
Stanford Res. Inst.
Menlo Park, Calif. 94026

Mr. R. Pilie
Cornell Aeronautical Lab., Inc.
P. O. Box 235
Buffalo, N. Y. 14214

Scientific & Tech. Info. Facility (25)
Attn: NASA Rep. (S-AK/RKT)
Box 33
College Park, Md.

Mr. Wm. Elam (2)
Bellcomm, Inc.
1100 17th St., N.W.
Washington, D. C.

Dr. Arnold Court
17168 Sept Street
Northridge, California

Commander
Hdqs., Air Weather Service
Scott AFB, Ill. 62225
Attn: Dr. Robert D. Fletcher
Library (2)

Office of Staff Meteorologist (2)
AFSC (SCWTS)
Andrews AFB
Washington, D. C. 20331

Air Force Systems Command
Space Systems Div.
Air Force Unit Post Office
Los Angeles, Calif. 90045

Meteorological & Geoastrophysical
Abstracts
P. O. Box 1736
Washington, D. C. 20013

Mr. Orville Daniel
PAWA/GMRD, AFMTC,
MU-235, Tech. Library
Patrick AFB, Fla. 32925

Martin-Marietta Corp.
Aerospace Div.
P. O. Box 179
Denver 1, Col.
Attn: Mr. J. M. Bidwell

Mr. Geo. Muller (FDTR)
Air Force Flt. Dyn. Lab.
Air Force Systems Command
Wright-Patterson AFB, Ohio

North American Aviation, Inc.
Space & Info. Sys. Div.
12214 Lakewood Blvd.
Downey, Calif. 90241
Attn: Mr. Clyde Martin

Dr. C. E. Buell
Karman Nuclear
Garden of the Gods Rd.
Colorado Springs, Colorado

Space Tech. Lab. Inc.
Structures Dept.
One Space Park
Redondo Beach, Calif.
Attn: Mr. M. White
Mr. Sol Lutwak

Mr. T. Y. Palmer
Res. Specialist, Aerospace Div.
Boeing Co., MS-23-81 656-PS88
P. O. Box 3703
Seattle, Wash.

Mr. Fred Martin
General Dynamics
5873 Kearny Village Rd.
San Diego, Calif.

Lockheed Co.
Sunnyvale, Calif. 94088
Attn: Dr. C. Boccius
Mr. H. Allison

National Center for Atmos. Res.
Boulder, Colorado 80302

Inst. for Env. Res.
ESSA
Boulder, Colorado

NASA - Kennedy Space Flt. Center
Mr. R. Jones
Dr. Knothe
Dr. Bruns
Mr. Keene
Mr. A. Taiani
Mr. Jelen
Mr. E. Ammon
Mr. Wilkinson
Library

NASA Headquarters
Federal Ofc. Bldg. No. 6
Washington, D. C. 20546
Attn: Technical Info. Div. (2)

Ofc. of Tracking & Data Acq.
Director

NASA Headquarters (Continued)

Office of Adv. Res. & Tech.
Director
Mr. M. Ames
Mr. F. Stephenson

Office of Space Science & Appl.
Director
Dr. M. Tepper
Mr. Spreen

Office of Manned Space Flt.
Mr. A. Kinny

NASA- Langley Res. Center
Langley Sta.
Hampton, Va. 23365
Attn: Director
Library
Mr. H. B. Tolefson
Mr. W. Reed, III

NASA-Goddard Space Flight Center
Greenbelt, Md. 20771
Attn: Mr. D. C. Kennard, Jr.
Technical Library

NASA-Lewis Res. Center
21000 Brookpark Rd.
Cleveland, Ohio 44135
Attn: Technical Library
Mr. H. Schmidt
Mr. J. Estes

NASA- Manned Spacecraft Center
Houston, Texas 77058
Attn: Director
Library
Mr. D. Wade (2)

NASA-Wallops Sta.
Wallops Island, Va. 23337
Attn: Director
Mr. J. Spurling

Army Missile Command
Redstone Arsenal, Ala. 35809
Attn: Dr. O. Essenwanger
Technical Library

DISTRIBUTION (CONT'D)

EXTERNAL (CONT'D)

Mr. H. D. Bagley
AMSMI-RRA, Bldg 5429
Physical Science Laboratory
Redstone Arsenal, Alabama 35809

Mr. A. L. Miller
AIR-5403
Naval Air Systems Command
Washington, D. C. 20360

Mr. R. M. Fenn
KXR, DoD Code 1232
U. S. Naval Weapons Laboratory
Dahlgren, Virginia 22448

Mr. H. Demboski
Code 421
Office of Naval Research
Washington, D. C. 20360

Capt T. H. R. O'Neill, USN
Naval Weather Service
Code 70
Washington (Navy Yard Annex)
Washington, D. C. 20390

Maj W. D. Kleis, USAF SCWT
Air Force Systems Command
Andrews AFB, Maryland 20331

LCOL F. J. Franz, USAF BSOW
Ballistics Systems Division
Norton AFB, California 92409

Mr. R. Leviton
CRER
Air Force Cambridge Research Lab
L. G. Hanscom Field
Bedford, Massachusetts 01731

Mr. V. S. Hardin
AWSAE
Air Weather Service
Scott AFB, Illinois 62226

Mr. C. A. Olson
Code 7261
Sandia Corporation, Sandia Base
Albuquerque, New Mexico 87110

Cdr W. S. Houston, Jr., USN
Chief, Environmental Sciences Div
Office of Asst Dir (Research)
OSD/Dept of Defense Rsch & Engr
Room 3E-1037, Pentagon
Washington, D. C. 20301

Dr. Robert White
Director, ESSA
1410 Gramax Building
8060 Thirteenth Street
Silver Springs, Maryland 20910

Dr. Karl R. Johannessen
Associate Director
U. S. Weather Bureau
1410 Gramax Building
8060 Thirteenth Street
Silver Springs, Maryland 20910

Col. Robert Long
Commanding Officer
Air Force Cambridge Research Labs
L. G. Hanscom Field
Bedford, Massachusetts 01731

The Boeing Co.
Space Division
Huntsville Industrial Center
Huntsville, Ala.
Attn: Mr. R. Wheeler
Mr. J. Hathorn (5)

Environmental Science Services Administration
National Severe Storms Laboratory
1616 Halley Avenue
Norman, Oklahoma 73069

DISTRIBUTION (CONT'D)

EXTERNAL (CONT'D)

R. A. Taft Sanitay Engineering Center
Public Health Service
4676 Columbia Parkway
Cincinnati, Ohio 45202

Meteorology Division
U. S. Army Dugway Proving Ground
Dugway, Utah 84022

B. N. Charles
Aerospace Corporation
P. O. Box 95085
Los Angeles, California 90045

Dr. H. Crutcher
ESSA
National Weather Records Center
Asheville, North Carolina 28801

Dr. Frank Gifford
Director, Atmospheric Diffusion Lab.
U. S. Weather Bureau, ESSA
Oakridge, Tennessee

Mr. R. K. Jenkins (SELWS-ER)
U. S. Army Electronic Research &
Development Activity
White Sands Missile Range, N. M
88002

Mrs. Norvella Billions
AMSMI-RRA
Redstone Arsenal, Alabama 35809

Mr. T. R. Carr
Code 3251, Box 22
Pacific Missile Range
Point Mugu, California 93041

Mr. N. J. Asbridge (WTWU)
Air Force Western Test Range
Vandenberg AFB, California 93437

LCOL R. F. Durbin, USAF WTW
Air Force Western Test Range
Vandenberg AFB, California 93437

Mr. Q. S. Dalton
Code 3069
Naval Ordnance Test Station
China Lake, California 93555

Mr. A. J. Krueger
Code 50
Naval Ordnance Test Station
China Lake, California 93555

LCOL B. F. Walker, USAF PCLW
Air Proving Ground Center
Eglin AFB, Florida 32542

Maj R. I. Vick, USAF PCCW
Air Proving Ground Center
Eglin AFB, Florida 32542

LCOL I. A. Van Brunt, USAF
WEA
Air Force Flight Test Center
Edwards AFB, California 93523

LCOL D. E. McPherson, Jr.
SSOTW
Air Force Satellite Control
Facility
Sunnyvale, California 94086

LCOL C. J. Loisel
SSSW
Hq, Space Systems Division
Los Angeles AF Station
Los Angeles, California 90045

Mr. K. C. Steelman
AMSEL-RD-SM
U. S. Army Electronic Research
& Development Laboratory
Fort Monmouth, New Jersey 07703